Phenomenological Analysis of Ground-State Bands in Even-Even Nuclei*

M. A. J. Mariscotti, Gertrude Scharff-Goldhaber, and Brian Buck
Brookhaven National Laboratory, Upton, New York

(Received 20 September 1968)

A *variable-moment-of-inertia* (VMI) *model* is proposed which permits an excellent fit of level energies of ground-state bands in even-even nuclei. In this model the energy of a level with angular momentum I is given by the sum of a potential energy term $\propto (\mathscr{I}_I - \mathscr{I}_0)^2$ (where $\mathscr{I}_0$ is the ground-state moment of inertia) and a rotational energy term $\hbar^2 I(I+1)/2\mathscr{I}_I$. It is required that the equilibrium condition $\partial E/\partial \mathscr{I} = 0$ be satisfied for each state. Each nucleus is described by two adjustable parameters, $\mathscr{I}_0$ and σ (the softness parameter), which are determined by a least-squares fit of all known levels. The calculated level energies and moments of inertia $\mathscr{I}_I$, $\mathscr{I}_0$, and σ are tabulated for 88 bands, ranging from Pd to Pt and from Th to Cm. Projections of three-dimensional arrays of $\mathscr{I}_0$ and σ on the (N, Z) plane are shown. These parameters are found to vary smoothly as function of N and Z. Breaks occur at $N=98$, 104, and 108. The osmium nuclei show a pronounced maximum for $\mathscr{I}_0$ and an equally pronounced minimum for σ at 108 neutrons. In Pt, $\mathscr{I}_0$ decreases steeply to 110 neutrons and then more slowly, while σ increases correspondingly. The stable Pt nuclei with $A=190$, 192, and 194 still possess appreciable moments of inertia and large but "finite" softness parameters. Hence they may be characterized as "pseudospherical." For nuclei exhibiting a near-harmonic level pattern (like Xe^{130}, Sm^{150}, and other neutron-deficient rare-earth isotopes), $\mathscr{I}_0$ becomes exceedingly small, but already for the 2+ state $\mathscr{I}$ is several orders of magnitude larger. The parameters of some $K=2$ bands in even-even nuclei and of bands found in odd-odd nuclei are related to those of appropriate ground-state bands in even-even nuclei. Evidence for a rotational band in Ir^{194} is deduced from recently published experimental results. A plot of E_4/E_2 versus A, presented for the discussion of the region of validity of the model, namely, $2.23 \leq E_4/E_2 < 3.33$, reveals new regularities. The empirical "Mallmann curves" (E_I/E_2 plotted versus E_4/E_2) are deduced from the VMI model within its region of validity. Graphs are presented which allow the determination of E_I (for $I \leq 16$) and of σ and $\mathscr{I}_0$ for each even-even nucleus for which the first 2+ and 4+ states are known. The model suggested by Harris, which includes the next-higher-order correction of the cranking model, is shown to be mathematically equivalent to the VMI model. The recently discovered appreciable quadrupole moments of 2+ states of "spherical nuclei" are compatible with the moments of inertia of these states given by the VMI model. The relation between $B(E2)(2'\to 2)/B(E2)(2\to 0)$ and E_4/E_2 is explored.

I. INTRODUCTION

We wish to show that the energy levels of the "ground-state bands" in even-even nuclei can be interpreted on the basis of a semiclassical model, in which the energy contains, in addition to the usual rotational term, a potential energy term which depends on the difference of the moment of inertia $\mathscr{I}_I$ (for the state with angular momentum I) from that of the ground state $\mathscr{I}_0$. We call this model the variable-moment-of-inertia (VMI) model.

We find that this simple two-parameter model, in which each nucleus is characterized by $(\mathscr{I}_0, \sigma)$, where σ is a "softness parameter," goes far in removing difficulties which have become apparent in recent years for various limiting models.

Since the level structure of even-even nuclei for the known ranges of Z and N shows, in spite of basic regularities, a great deal of variation, it seems appropriate to survey the situation in some detail before introducing the model: We shall start with rotational bands which represent a special case of the ground-state bands. As is well known, rotational bands occur in nuclei which may be described as strongly deformed spheroids rotating about an axis perpendicular to their axis of symmetry.[1] For these nuclei the adiabatic condition is fulfilled, which stipulates that the energies of vibrations and the energies necessary to split nucleon pairs appreciably exceed the rotational energy. In this case the energy of the rotational level with angular momentum I is given by

$$E_I = \tfrac{1}{2}\hbar^2[I(I+1)/\mathscr{I}] \tag{1}$$

($I=2, 4, 6, \cdots$; even parity). We can thus describe the "rotational structure" of each nucleus with one parameter, the moment of inertia $\mathscr{I}$. $\mathscr{I}$ is known to increase markedly with the deformation parameter β. In order to take a moderate amount of rotation-vibration mixing into account, one can write[1]

$$E = AI(I+1) - BI^2(I+1)^2, \tag{2}$$

where $B/A \lesssim 10^{-3}$. Nuclei with rotational bands occur for $150 \leq A \leq 186$, $A \geq 224$, in the most neutron-deficient Ba nuclei, and again in the regions around Mg^{24}, C^{12}, and Be^8. The onset of the deformed "rare earths" region is quite abrupt at 90 neutrons,[2] and the onset of the deformed "heavy element" region occurs at 88 protons.[3]

The spheroidal model gives the intraband reduced transition probability[1] (i.e., the transition probability within the rotational band built on the ground state

* Work performed under the auspices of the U.S. Atomic Energy Commission.

[1] A. Bohr and B. R. Mottelson, Kgl. Danske Videnskab. Selskab, Mat.-Fys. Medd. **27**, No. 16 (1953).

[2] G. Scharff-Goldhaber and J. Weneser, Phys. Rev. **98**, 212 (1955).

[3] Gertrude Scharff-Goldhaber, Phys. Rev. **103**, 837 (1956).

for the γ transition $I+2\rightarrow I$) by

$$B(E2)=\frac{15}{32\pi}e^2Q^2\frac{(I+1)(I+2)}{(2I+3)(2I+5)}, \qquad (3)$$

where Q is the intrinsic quadrupole moment. The $2+\rightarrow 0+$ transitions are known to be enhanced up to 200 times compared to single-particle transitions.[4] Until very recently, only the transition probabilities between $4+\rightarrow 2+$ and $2+\rightarrow 0+$ had been measured.[5] The ratio $B(E2)(4\rightarrow 2)/B(E2)2\rightarrow 0)$ agrees very well with the model prediction given by Eq. (3). More recent Coulomb excitation and reaction experiments using a Doppler shift method show[6] that also the transitions $6+\rightarrow 4+$ and $8+\rightarrow 6+$ are at least as enhanced as Eq. (3) would predict.

Between the strongly deformed and "magic number" nuclei are found the nuclei with a near-harmonic pattern,[2] which is characterized by a second excited state with an energy approximately twice the energy of the first excited state and $I=0$, 2, or 4. (The second excited $2+$ state is usually denoted by $2'+$.) In these nuclei the $2+\rightarrow 0+$ transitions as well as the $4+\rightarrow 2+$, $0'+\rightarrow 2+$, and the $E2$ part of the $2'+\rightarrow 2+$ transitions are enhanced up to 40 or 50 times compared to single-particle transitions, whereas the $2'+\rightarrow 0+$ transitions are retarded. These features are successfully described by the spherical model.[2] However, recently it was found that the $2+$ states of some of the near-harmonic nuclei have sizeable intrinsic quadrupole moments,[7] in disagreement with the spherical model predictions. Also, the model predicts

$$B(E2)(2'\rightarrow 2)/B(E2)(2\rightarrow 0)=2,$$

while most of the experimental values are appreciably smaller.[8–12] Another difficulty is encountered in the Pt nuclei: While the model predicts $E_{2'}/E_2\geq 2$, these values for Pt^{192}, Pt^{194}, and Pt^{196} are 1.93, 1.89, and 1.94, respectively.

A gradual transition between the level patterns of rotational nuclei and near-harmonic nuclei was first observed in the even-even osmium nuclei.[13,14] These nuclei have bands with the spin sequence 0, 2, 4, 6, 8, $\cdots$, and even parity, whose level energies increase as the neutron number increases, while simultaneously the γ-vibrational energy decreases. Consequently, the adiabatic condition does not hold any more. The energy ratios of the ground-state band deviate more and more from the $I(I+1)$ rule as N increases, and cannot be fitted by means of moderate rotation-vibration mixing [Eq. (2)]. However, fairly satisfactory two-parameter fits are obtained using the Davydov-Filippov[15] asymmetric model. In this description the axial asymmetry increases from $\gamma=16°$ to 25° between Os^{186} and Os^{192}. The parameter γ is simply related to $E_{2'}/E_2$, the energy ratio of the second and first $2+$ states. A study of the branching ratios between the γ-vibrational ($K=2$) and the ground-state bands in the framework of the same model yields values of γ ranging from 12° to 23° for the same nuclei, suggesting a small inconsistency in the axially asymmetric model not easily removed by more sophisticated approaches.[14]

It was further shown by Mallmann[16] that for even-even nuclei with widely differing N, Z, and E_2 values the energy ratios E_6/E_2 and E_8/E_2, plotted against E_4/E_2, lie on two "universal" curves. This finding suggests that these ground-state bands may indicate features of nuclear dynamics which are common to nuclei both in the deformed and in the near-harmonic region.

A powerful new method for populating ground-state bands in neutron-deficient nuclei by means of the (α, $2n$) and (α, $4n$) reactions was developed by Morinaga and Gugelot.[17] In some cases states with angular momentum 10 or 12 were populated in this way.[17–20] This method made use of the large amount of angular momentum imparted to the nucleus by the incoming α particle. The method was extended to heavier ions,[21–25] up to Ar.[26] Thus, ground-state bands in nuclei in the near-harmonic region [e.g., in Xe, Ba, and Ce ($120\leq A\leq 136$) and in Pt ($182\leq A\leq 194$)] and/or far off stability were populated. In some cases, states up to $18+$ were reached. Some typical examples of such bands are given in Fig. 1. In all cases the energy spacings at higher I are smaller than required by the $I(I+1)$ rule. Again the higher levels cannot be fitted by Eq. (2).

[4] Paul H. Stelson and Lee Grodzins, Nucl. Data **A1**, 21 (1965).
[5] A. C. Li and A. Schwarzschild, Phys. Rev. **129**, 2664 (1963).
[6] R. M. Diamond, M. M. Kelly, F. S. Stephens, and D. Ward (private communication).
[7] J. de Boer and J. Eichler, Advan. Nucl. Phys. **1**, 1 (1968), and references therein.
[8] P. H. Stelson and F. K. McGowan, Phys. Rev. **121**, 209 (1961).
[9] F. K. McGowan and P. H. Stelson, Phys. Rev. **126**, 257 (1962).
[10] F. K. McGowan, R. L. Robinson, P. H. Stelson, and J. L. C. Ford, Jr., Nucl. Phys. **66**, 97 (1965).
[11] W. T. Milner, F. K. McGowan, R. L. Robinson, P. H. Stelson, and R. O. Sayer, Bull. Am. Phys. Soc. **12**, 1201 (1967).
[12] F. K. McGowan, R. L. Robinson, P. H. Stelson, and W. T. Milner, Nucl. Phys. **A113**, 529 (1968).
[13] G. Scharff-Goldhaber, in Proceedings of the University of Pittsburgh Conference, 1957, p. 447 (unpublished).
[14] G. T. Emery, W. R. Kane, M. McKeown, M. L. Perlman, and G. Scharff-Goldhaber, Phys. Rev. **129**, 2597 (1963).
[15] A. S. Davydov and C. F. Filippov, Nucl. Phys. **8**, 237 (1958).
[16] C A. Mallmann, Phys. Rev. Letters **2**, 507 (1959).
[17] H. Morinaga and P. C. Gugelot, Nucl. Phys. **46**, 210 (1963).
[18] N. Lark and H. Morinaga, Nucl. Phys. **63**, 466 (1965).
[19] H. Morinaga and N. Lark, Nucl. Phys. **67**, 315 (1965).
[20] H. Morinaga, Nucl. Phys. **75**, 385 (1966).
[21] F. S. Stephens, N. Lark, and R. M. Diamond, Phys. Rev. Letters **12**, 225 (1964).
[22] F. S. Stephens, N. L. Lark, and R. M. Diamond, Nucl. Phys. **63**, 82 (1965).
[23] J. Burde, R. M. Diamond, and F. S. Stephens, Nucl. Phys. **A92**, 306 (1967).
[24] T. E. Clarkson, R. M. Diamond, F. S. Stephens, and I. Perlman, Nucl. Phys. **A93**, 272 (1967).
[25] J. O. Newton, F. S. Stephens, and R. M. Diamond, Nucl. Phys. **A95**, 357 (1967).
[26] F. S. Stephens, D. Ward, and J. O. Newton, J. Phys. Soc. Japan Suppl. **24**, 160 (1968).

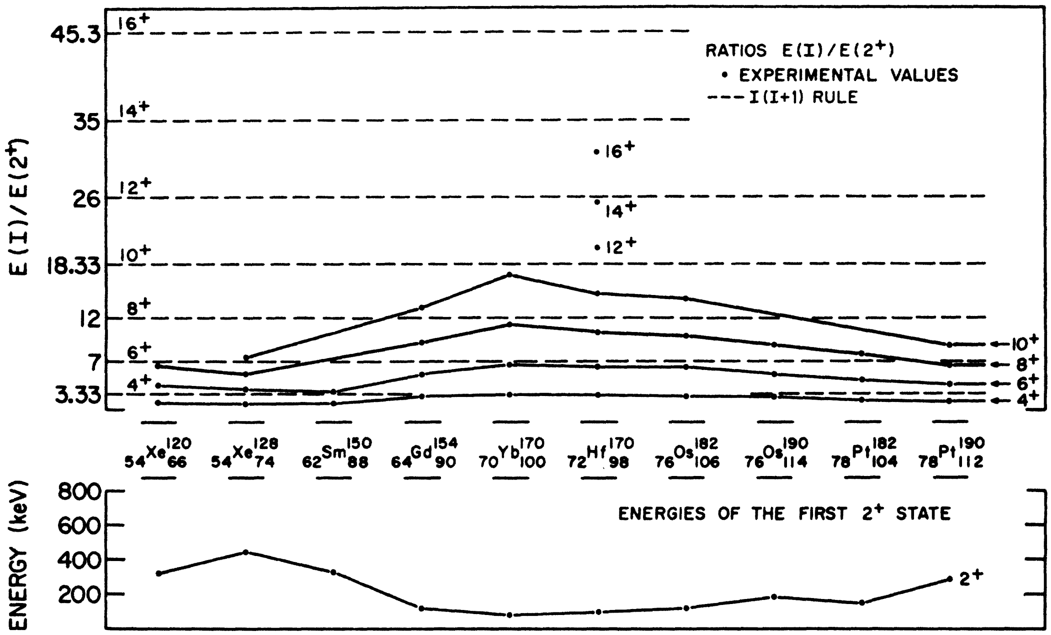

FIG. 1. Energy ratios E_I/E_2 (above) and energies E_2 (below) for some even-even nuclei. The horizontal dashed lines indicate the values given by the $I(I+1)$ rule. The deviations from this rule increase as nuclei become less deformed. Simultaneously the energy of the first 2+ state increases.

Since $E=\hbar^2 I(I+1)/2\mathcal{I}$ for rotational bands, this decrease in energy spacing may be attributed to an increase in the moment of inertia $\mathcal{I}$. At large I the moment of inertia appears to approach the "rigid" value. Morinaga[20] proposed the term "softness" for the percentage increase of the moment of inertia per unit change of angular momentum, $\Delta\mathcal{I}/\mathcal{I}\Delta I$, and discussed the form of the dependence of this quantity on I as a function of N and Z.

Three different explanations for the increase of the moment of inertia have been proposed: (a) At higher angular momenta the deformation (β) increases (β stretching)[27]; (b) the pairing energy for neutrons and protons decreases with increasing I[28]; and (c) an extension of the cranking model to higher-order terms in the nuclear angular velocity ω leads to an increase of $\mathcal{I}$ with increasing I.[29]

The semiclassical model[27] based on assumption (a) leads to an expression of the energy of the state as the sum of a potential energy term and a kinetic (rotational) energy term:

$$E_I(\beta)=\tfrac{1}{2}C(\beta_I-\beta_0)^2+[I(I+1)/2\mathcal{I}(\beta_I)], \quad (4)$$

where $\mathcal{I}$ is the moment of inertia in units of $\hbar^2$. Further, the equilibrium condition $\partial E_I/\partial\beta_I=0$ is applied to obtain the value of β_I. With this model a good fit may be obtained for bands of strongly deformed nuclei, assuming the relation given by the hydrodynamical model $\mathcal{I}\sim\beta^2$. However, bands outside the deformed region cannot be fitted by this method with reasonable accuracy.[27]

Another difficulty for this model arose when recent studies of muonic x rays and of isomer shifts observed by the Mössbauer effect[30,31] indicated that the increase in β is not large enough to explain the deviations from the $I(I+1)$ rule. These results obtained support from theoretical considerations[32] which showed that the decrease of the effective pairing force [assumption (b)] has an even greater influence on the increase of the moment of inertia with increasing I than the increase of deformation. These findings suggest that a more realistic treatment of ground-state bands should include more degrees of freedom than just β. However, in view of the lack of detailed knowledge of the changes in nuclear structure as a function of I and in view of the sweeping regularities[16] displayed by the ground-state bands, the following approach was taken[33]: The defor-

[27] R. M. Diamond, F. S. Stephens, and W. T. Swiatecki, Phys. Letters **11**, 315 (1964).
[28] B. R. Mottelson and J. G. Valatin, Phys. Rev. Letters **5**, 511 (1960).
[29] S. H. Harris, Phys. Rev. **138**, B509 (1965).
[30] S. Bernow, S. Devons, I. Duerdoth, D. Hitlin, J. W. Kast, E. R. Macagno, J. Rainwater, K. Runge, and C. S. Wu, Phys. Rev. Letters **18**, 787 (1967); D. Yeboah-Amankwah, L. Grodzins, and R. Frankel, *ibid.* **18**, 791 (1967).
[31] E. R. Marshalek, Phys. Rev. Letters **20**, 214 (1968).
[32] D. R. Bes, S. Landowne, and M. A. J. Mariscotti, Phys. Rev. **166**, 1045 (1968).
[33] M. Mariscotti, Brookhaven National Laboratory Report No. BNL-11838, 1967 (unpublished).

mation parameter β was replaced by a general variable x in Eq. (4) and it was assumed that the moment of inertia can be expressed by $\mathscr{I}\approx x^n$, n being an integer. Since the best fits for all ground-state bands—those of the strongly deformed nuclei as well as of the near-spherical nuclei—were obtained for $n=1$,[33] it became evident that the moment of inertia $\mathscr{I}$ itself may be considered as the general variable x. Thus one arrives at the VMI model referred to in the beginning:

The level energy is given by

$$E_I(\mathscr{I})=\tfrac{1}{2}C(\mathscr{I}-\mathscr{I}_0)^2+\tfrac{1}{2}[I(I+1)/\mathscr{I}], \qquad (5)$$

and the equilibrium condition

$$\partial E(\mathscr{I})/\partial\mathscr{I}=0 \qquad (6)$$

determines the moment of inertia $\mathscr{I}_I$ (given in units of $\hbar^2$) for each state with spin I. $\mathscr{I}_0$ is a parameter defined as the "ground-state moment of inertia" and C is the "restoring force constant."[33,34]

The VMI model is remarkably successful in

(a) justifying Mallmann's empirical curves (Sec. II C);

(b) going beyond the range of validity of the asymmetric model toward the "spherical" region (Sec. II B);

(c) showing, through the two model parameters, the general smooth change in the structure of even-even nuclei as a function of Z and N, as well as small superimposed "breaks" or extrema which may be related to the properties of the corresponding Nilsson orbits (Sec. III A);

(d) predicting levels of ground-state bands (Secs. II C and III A);

(e) correlating properties which contradict the spherical model [e.g., the large electric quadrupole moments found via the reorientation effect for 2+ states (Sec. III C) and the anomalies found in Pt nuclei (Sec. III A)] with the VMI $\mathscr{I}$; and

(f) fitting, in addition, rotational bands built on γ-vibrational states in even-even nuclei and rotational bands in odd-odd nuclei (Sec. III B).

It is further shown that the next higher order of the cranking-model approach suggested by Harris[29] is mathematically equivalent to the VMI model (Sec. II D). As was pointed out by Stephens, Ward, and Newton,[26] other published two-parameter fits are either less good than Harris's, and hence than the one proposed here, or limited to the strongly deformed region.

The VMI model proposed here is independent of the contributions of various factors to the increase in moment of inertia with increasing I, such as β stretching and decrease in pairing energy. However, in Sec. III C it will be shown that in the framework of this model the empirical relation of deformation and moment of inertia may be studied more meaningfully than was hitherto possible.

[34] G. Scharff-Goldhaber, J. Phys. Soc. Japan Suppl. **24**, 150 (1968).

II. FORMULATION AND FRAMEWORK OF THE VMI DESCRIPTION

A. General Solution and Parameters

For each spin I there exists an equilibrium value of the variable $\mathscr{I}$, the moment of inertia of the nucleus determined by the condition (6). From (5) and (6) we obtain

$$\mathscr{I}_I=\mathscr{I}_0/\{1-[I(I+1)/2C\mathscr{I}_I^3]\}, \qquad (7)$$

which is equivalent to the cubic equation

$$\mathscr{I}_I^3-\mathscr{I}_I^2\mathscr{I}_0-[I(I+1)/2C]=0. \qquad (8)$$

This cubic equation has one real root for any finite positive value of $\mathscr{I}_0$ and C and can be solved algebraically.

Equation (7) combined with Eq. (5) yields the following expression for the energy of the state with spin I:

$$E_I=[I(I+1)/2\mathscr{I}_I]\{1+[I(I+1)/4C\mathscr{I}_I^3]\}, \qquad (9)$$

which involves two parameters: $\mathscr{I}_0$ and C. These two parameters characterize each nucleus defining the moments of inertia $\mathscr{I}_I$ [Eqs. (7) or (8)] and the energies E_I [Eq. (9)] of the states of the ground-state band. Both $\mathscr{I}_I$ and E_I are increasing functions of I. The "softness," i.e., the relative increase of the moment of inertia with angular momentum I [similar to the quantity $(1/\mathscr{I})\Delta\mathscr{I}/\Delta I$ introduced by Morinaga[20]] can be derived from Eq. (8):

$$\mathscr{I}^{-1}(d\mathscr{I}/dI)=[(2I+1)/2C\mathscr{I}^2(3\mathscr{I}-2\mathscr{I}_0)]. \qquad (10)$$

For the particular case $I=0$ we obtain

$$\sigma=[\mathscr{I}^{-1}(d\mathscr{I}/dI)]_{I=0}=1/2C\mathscr{I}_0^3. \qquad (11)$$

The quantity σ provides a measure of the softness of the nucleus and is particularly useful in discussing the properties of the present model as well as in permitting a more meaningful two-parameter identification of each nucleus (see below).

B. Range of Validity of the VMI Model

In order to determine the limits of validity of this semiclassical approach we define $r_I=\mathscr{I}_I/\mathscr{I}_0$ and, by dividing Eq. (8) by $\mathscr{I}_0^3$, we obtain

$$r_I^3-r_I^2=\sigma I(I+1). \qquad (12)$$

In the adiabatic limit, $\sigma=0$, and hence $r_I=1$. Equation (9) then assumes the well-known form given by Eq. (1)

$$E_I(\sigma=0)=I(I+1)/2\mathscr{I}_0.$$

In this limit, the energy ratio $R_I=E_I/E_2$ is

$$R_I(\sigma=0)=\tfrac{1}{6}I(I+1). \qquad (13)$$

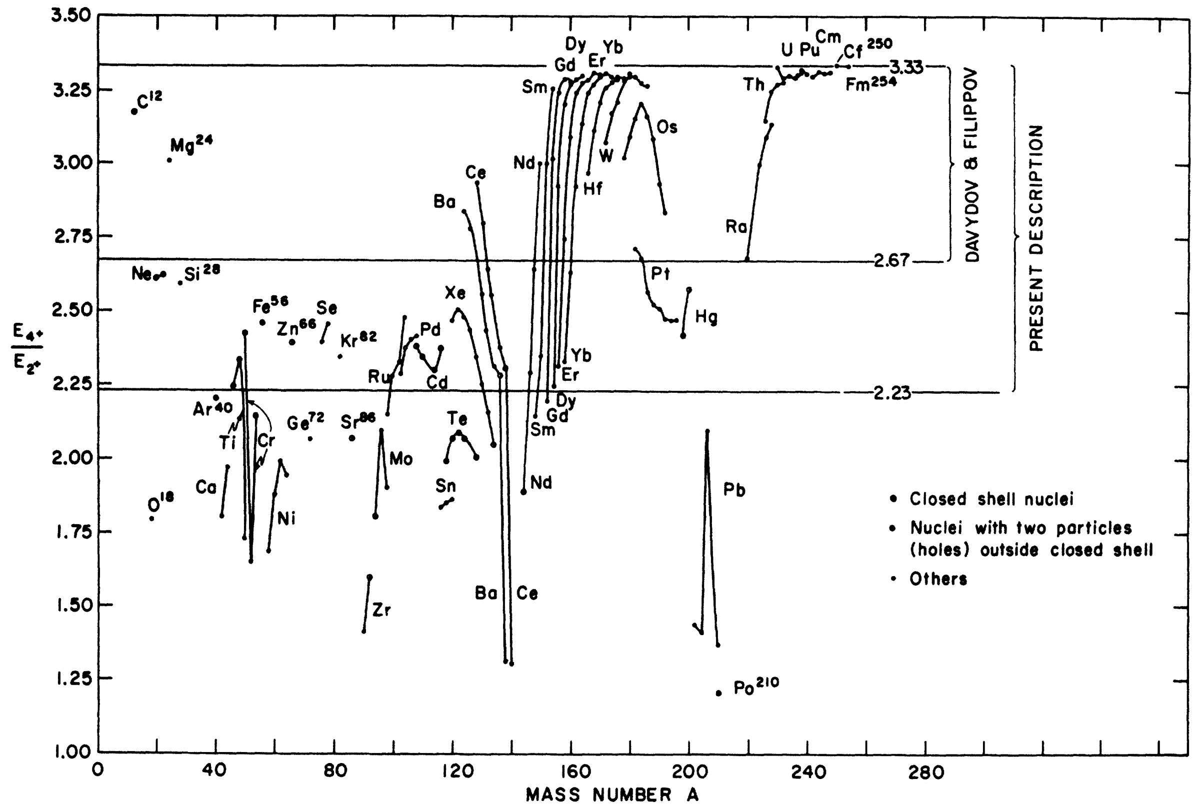

FIG. 2. Experimental values of E_4/E_2 (ratio of energy of the first 4+ state to the energy of the first 2+ state) in even-even nuclei. The horizontal line at the top indicates the value given by the $I(I+1)$ law. The interval $2.67<E_4/E_2<3.33$ corresponds to the predictions of the asymmetric rotor model of Davydov and Filippov. Ratios in the interval $2.23<E_4/E_2<3.33$ lie within the limits of the present description, which is successful in fitting the known ground-state bands of nuclei in this interval. Most of the nuclei below $E_4/E_2=2.23$ have no more than two particles (holes) outside a single closed shell.

On the other hand, in the limit of very soft nuclei, $\sigma\rightarrow\infty$, and from Eq. (12) we obtain $r_I=[\sigma I(I+1)]^{1/3}$. Equation (9) then becomes

$$E_I(\sigma\rightarrow\infty)=\tfrac{3}{4}[I(I+1)/\mathcal{J}_I],$$

which leads to the following expression for the energy ratio R_I in this limit:

$$\begin{aligned}R_I(\sigma\rightarrow\infty)&=\tfrac{1}{6}I(I+1)(\mathcal{J}_2/\mathcal{J}_I)\\&=I(I+1)r_2/6r_I\\&=[\tfrac{1}{6}I(I+1)]^{2/3}.\end{aligned}\qquad(14)$$

Equations (13) and (14) now permit us to define the range of validity of the VMI description in terms of the energy ratios, as follows:

$$[\tfrac{1}{6}I(I+1)]^{2/3}\leq R_I\leq\tfrac{1}{6}I(I+1).\qquad(15)$$

In the case $I=4$, Eq. (14) gives the value

$$R_4(\sigma\rightarrow\infty)=(10/3)^{2/3}\cong2.23,$$

while the adiabatic or "strong coupling" value given by Eq. (13) is

$$R_4(\sigma=0)=10/3\cong3.33.$$

The interval defined by Eq. (15) is thus larger than that given by the Davydov-Filippov model,[15] where $3.33>R_4>8/3\approx2.67$.[35] These intervals are graphically compared in Fig. 2 for $I=4$. This figure shows a plot of R_4 for all even-even nuclei for which at least one 4+ state is known.[36–39] (In every case the first 4+ excited state has been used to evaluate R_4.) The strong-coupling limit of 3.33, which is approached by the well-deformed

[35] C. A. Mallmann and A. K. Kerman, Nucl. Phys. **16**, 105 (1960).
[36] Nucl. Data **B1** (1966).
[37] C. M. Lederer, J. M. Hollander, and I. Perlman, *Table of Isotopes* (John Wiley & Sons, Inc., New York, 1967), 6th ed.
[38] M. Neiman and David Ward, University of California Radiation Laboratory Report No. UCRL-17989, 1967, p. 22 (unpublished).
[39] D. Ward, R. M. Diamond, and F. S. Stephens, Nucl. Phys. **A117**, 309 (1968).

nuclei, is indicated with a horizontal line at the top of the figure. The second line at $R_4=2.67$ indicates the lower limit given by the Davydov-Filippov model. It is seen that the nuclei in the heavy-element region, most of the rare-earth nuclei, two Ba isotopes, and two Ce isotopes lie within the range of the asymmetric rotor description. There are, however, several nuclei outside this range for which well-established ground-state bands have recently been found such as the $Xe^{120-130}$ isotopes, $Ce^{132-136}$, Dy^{154}, Er^{156}, $Yb^{158,160}$, and $Pt^{186-194}$, which are seen to be included in the present description.

In addition to these nuclei, many others are known from decay scheme studies to have $R_4>2.23$, but only in a few cases (e.g., Pd^{108} and Cd^{110}) is a $6+$ state known. As will be shown in Sec. III, all these nuclei with three

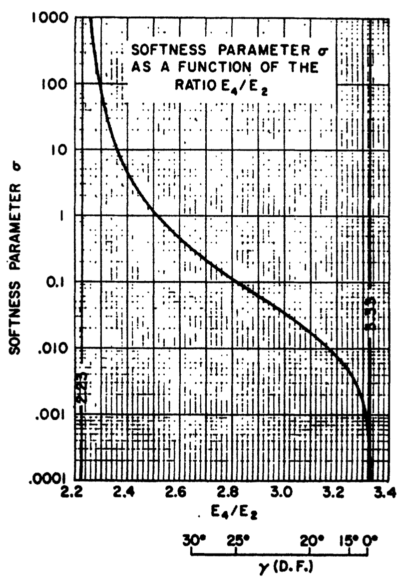

FIG. 3. Softness parameter σ as a function of the E_4/E_2 ratio (see Sec. II C). Also shown are the corresponding values of the parameter γ according to the asymmetric rotor model of Davydov and Filippov.

or more known members of the ground-state band have been successfully fitted by the present description. Most of the nuclei with $R_4<2.23$ are within two particles (holes) from a closed shell.

The regularity of R_4 values discernible from this figure is remarkable. If both $2+$ and $4+$ states are known for several isotopes of one element, R_4, in most cases, is seen to ascend to a maximum value and to descend again. It is noteworthy that for Cd, where several isotopes are known to have almost ideal spherical level patterns, this trend is reversed.

C. Energy Ratios and Parameters as Functions of R_4

In Sec. III the results of the least-squares-fitting procedure used to compute the level energies E_I, the

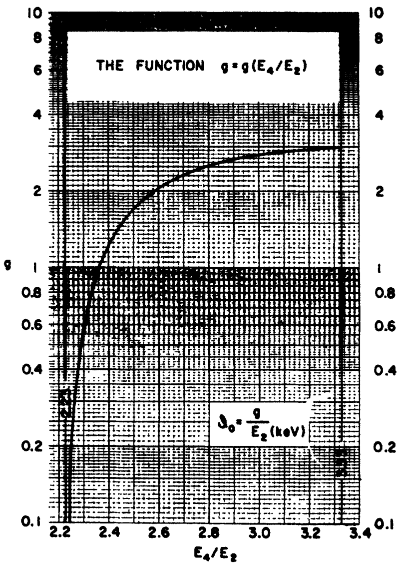

FIG. 4. Function $g=g(E_4/E_2)$ which relates the ground-state moment of inertia $\mathcal{J}_0$ with the energy of the first $2+$ state.

moments of inertia $\mathcal{J}_I$, and the parameters $\mathcal{J}_0$ and C, or, alternatively, σ, will be presented. However, since the solution of Eq. (8) is somewhat involved, it is sometimes useful to derive the energy of upper levels and the corresponding values of the parameters simply from the ratio R_4 and the energy of the first excited state E_2.

To show the relationship between R_4 and σ, $\mathcal{J}_0$, and R_I, we write Eq. (9) in terms of $r_I=\mathcal{J}_I/\mathcal{J}_0$:

$$E_I=[I(I+1)/4\mathcal{J}_0][(3r_I-1)/r_I^2], \qquad (16)$$

and obtain

$$R_I=\tfrac{1}{6}I(I+1)[(3r_I-1)r_2^2/(3r_2-1)r_I^2]. \qquad (17)$$

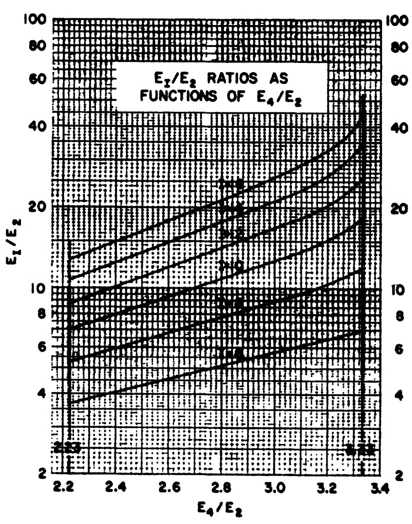

FIG. 5. Energy ratios E_I/E_2 as functions of E_4/E_2 as predicted by the VMI model.

Equation (17) depends only on one parameter, the softness parameter σ, since r_I is a solution of Eq. (12). For a given I, R_I can be shown to be a single-valued function of σ (for $\sigma > 0$), and therefore a given value of R_4 fixes the parameter σ. Figure 3 shows a graphical representation of the function $\sigma = \sigma(R_4)$ which can be used to deduce the softness parameter when R_4 is known.

If both R_4 and E_2 are known, the value of the parameter $\mathscr{I}_0$ can be obtained from Eq. (16):

$$\mathscr{I}_0 = g/E_2, \tag{18}$$

where

$$g = 1.5[(3r_2 - 1)/r_2^2].$$

The quantity g is, again, only a function of σ, and therefore of R_4. This function, $g = g(R_4)$, is shown in Fig. 4.

Finally, Eq. (17), which gives R_I as a function of σ, can be used to evaluate R_I in terms of R_4. Thus the energies of upper members of the band can be obtained from R_4 and E_2 alone. Figure 5 shows the function $R_I = R_I(R_4)$ for $6 \le I \le 16$.

As mentioned in the Introduction, the experimental evidence for the two lowest curves, $I = 6$ and 8, shown in Fig. 5, was first presented by Mallmann.[16]

D. Equivalence of the Harris and VMI Models

Harris[29] has shown that an extension of the cranking model to the next order of perturbation theory in the angular velocity ω leads to a very good agreement with experimental data on rotational bands of even-even nuclei in the rare-earth region. Although the (two-parameter) Harris model and the present description appear, at least *a priori*, to be completely unrelated, both lead, surprisingly, to the same expression for the level energy E_I, as is shown below.

The two-parameter Harris model reduces to the two equations:

$$[I(I+1)]^{1/2} = \omega(\mathscr{I}_0' + 2C'\omega^2), \tag{19}$$

$$E_I' = \tfrac{1}{2}(\mathscr{I}_0' + 3C'\omega^2)\omega^2, \tag{20}$$

which permit the elimination of ω and give the level energy E_I' in terms of the two parameters $\mathscr{I}_0'$ and C'.

If the moment of inertia $\mathscr{I}_I$ is defined as

$$\mathscr{I}_I = [I(I+1)]^{1/2}/\omega, \tag{21}$$

one obtains, from Eq. (19),

$$\begin{aligned}\mathscr{I}_I &= \mathscr{I}_0' + 2C'\omega^2 \\ &= \mathscr{I}_0' + 2C'[I(I+1)/\mathscr{I}_I^2]\end{aligned} \tag{22}$$

or, equivalently,

$$\mathscr{I}_I^3 - \mathscr{I}_I^2\mathscr{I}_0' - 2C'I(I+1) = 0, \tag{23}$$

which is identical to Eq. (8) if

$$C' = 1/4C \quad \text{and} \quad \mathscr{I}_0' = \mathscr{I}_0. \tag{24}$$

Using Eqs. (22) and (24), Eq. (20) can then be written

$$E_I' = \tfrac{1}{2}(\mathscr{I}_I + C'\omega^2)\omega^2.$$

Substituting ω from Eq. (21), we obtain

$$\begin{aligned}E_I' &= \tfrac{1}{2}\{\mathscr{I}_I + C'[I(I+1)/\mathscr{I}_I^2]\}[I(I+1)/\mathscr{I}_I^2] \\ &= I(I+1)/2\mathscr{I}_I\{1 + C'[I(I+1)/\mathscr{I}_I^3]\}.\end{aligned} \tag{25}$$

Using the relations (24), one finds that Eq. (25) is identical with Eq. (9).

III. CALCULATIONS AND RESULTS

A. Analysis of Ground-State Bands of Even-Even Nuclei

We have evaluated the level energies E_I, Eq. (9), for the 88 nuclei listed in Table I, up to spin $I = 16$. The two parameters $\mathscr{I}_0$ and C were determined by means of a least-squares fitting procedure involving all the experimentally known level energies. Because of the frequently encountered difficulty of assigning the correct error to the experimental values reported in the literature, we have chosen to weight each energy value by the square of its inverse, which is equivalent to assuming a constant relative error.

Our analysis included all nuclei with at least three known excited states of the ground-state band whose energies satisfied Eq. (15). The results are presented in Table I. For each nucleus the first row in Table I contains the experimental energies and their errors. The values shown in parentheses indicate data reported as doubtful and not taken into account for the fitting procedure. The second and third rows give the level energies and moments of inertia, respectively, obtained by fitting Eq. (9) to the experimental data shown above. The values of $\mathscr{I}_0$, C, and σ obtained for each nucleus are given in Table II.

A graphical comparison of the experimental and calculated energies of some even-even nuclei is also presented in Fig. 6, where for each case the experimental level energies are shown on the left and the calculated values are shown on the right. It is seen that in most cases there is agreement within the experimental errors.

In Fig. 7 we have plotted $\mathscr{I}_0$ as a function of Z and N for all nuclei listed in Table I. In addition, the values for the Ra isotopes are plotted, for which only 2+ and 4+ states are known. A similar tridimensional plot is presented in Fig. 8, where the softness parameter σ for each nucleus is shown.

The Pd, Cd, Xe, Ba, and Ce isotopes nearest closed neutron shells are among the nuclei with the smallest ground-state moments of inertia (Fig. 7), as well as among the softest (Fig. 8).

The ground-state moments of inertia as well as the softness parameters σ obtained for the Sm and Gd isotopes (Figs. 7 and 8) clearly show the transition

TABLE I. Experimental and calculated energies and moments of inertia of levels of ground-state bands of even-even nuclei. For each nucleus the first row contains the experimental energies with the reported errors. The values shown in parentheses indicate values reported as doubtful and not taken into account in the least-squares fit. The second and third rows give the energies and moments of inertia obtained with the VMI model for levels with angular momentum $2 \leq I \leq 16$.

I	2	4	6	8	10	12	14	16
Pd^{108}								
E_{expt}[a]	433.8±1	1047.5±1.5	1770.0±5					
E	434.0	1045.0	1772.8	2590.4	3482.4	4438.6	5451.5	6515.8
$\mathcal{J}$	0.0093	0.0133	0.0168	0.0198	0.0227	0.0254	0.0279	0.0303
Cd^{110}								
E_{expt}[b]	657.72±0.05	1542.3±0.1	2479.6±0.5					
E	661.4	1513.5	2510.0	3618.9	4821.6	6105.6	7461.9	8883.6
$\mathcal{J}$	0.0066	0.0097	0.0123	0.0147	0.0169	0.0189	0.0209	0.0227
Xe^{120}								
E_{expt}[c]	321.8±1	794.4±2	1396±3	2097±4	(2870)			
E	319.4	807.0	1399.6	2072.0	2810.0	3604.5	4448.8	5338.0
$\mathcal{J}$	0.0119	0.0165	0.0205	0.0241	0.0274	0.0305	0.0335	0.0362
Xe^{122}								
E_{expt}[c]	331.1±1	828.6±2	1467±3	2217±4	(3036)			
E	328.4	842.6	1471.8	2188.3	2976.3	3825.8	4729.6	5682.2
$\mathcal{J}$	0.0114	0.0156	0.0193	0.0226	0.0256	0.0285	0.0312	0.0339
Xe^{124}								
E_{expt}[d]	355±10	880±12	1555±15	2355±20				
E	351.8	897.2	1562.7	2319.3	3150.8	4046.7	4999.3	6003.1
$\mathcal{J}$	0.0107	0.0147	0.0182	0.0214	0.0243	0.0270	0.0296	0.0321
Xe^{126}								
E_{expt}[d]	390±10	950±10	1645±15	2445±20				
E	388.0	959.9	1648.4	2426.1	3277.3	4191.9	5162.4	6183.4
$\mathcal{J}$	0.0101	0.0142	0.0177	0.0208	0.0238	0.0265	0.0291	0.0316
Xe^{128}								
E_{expt}[d]	444±5	1041±10	1745±15	2531±20	3391±20			
E	443.8	1041.0	1745.4	2532.8	3389.2	4305.2	5274.2	6290.9
$\mathcal{J}$	0.0095	0.0137	0.0174	0.0207	0.0237	0.0265	0.0292	0.0318
Xe^{130}								
E_{expt}[d,e]	534±8	1203±10	1951±15	2785±20	(3710)			
E	534.2	1192.4	1955.7	2801.4	3716.3	4691.1	5719.4	6796.1
$\mathcal{J}$	0.0084	0.0126	0.0161	0.0193	0.0222	0.0250	0.0276	0.0300
Ba^{134}								
E_{expt}[c]	229.5±1	650.6±2	1223±3	(1857)				
E	228.7	656.8	1215.2	1872.0	2608.9	3414.3	4279.6	5198.7
$\mathcal{J}$	0.0145	0.0180	0.0213	0.0243	0.0272	0.0299	0.0324	0.0350

TABLE I (*Continued*)

I	2	4	6	8	10	12	14	16
Ba^{126}								
$E_{expt}{}^{c}$	256.1±1	711.6±2	1333±3	2090±4	(2919)			
E	253.4	725.1	1339.0	2060.2	2868.8	3751.9	4700.5	5707.6
$\mathscr{J}$	0.0131	0.0164	0.0194	0.0222	0.0248	0.0273	0.0297	0.0319
Ce^{128}								
$E_{expt}{}^{f}$	207.3	607.3	1157.8	1820.0	(2573)			
E	206.2	613.1	1158.6	1809.7	2547.2	3358.2	4233.6	5166.7
$\mathscr{J}$	0.0156	0.0186	0.0216	0.0244	0.0271	0.0296	0.0320	0.0344
Ce^{130}								
$E_{expt}{}^{f}$	254.1	710.7	1324.1	2053.1				
E	252.4	719.5	1325.7	2036.8	2833.4	3702.8	4636.3	5627.1
$\mathscr{J}$	0.0132	0.0165	0.0196	0.0225	0.0252	0.0277	0.0301	0.0324
Ce^{132}								
$E_{expt}{}^{f}$	325.4	858.9	1542.7	2331.0				
E	324.1	865.9	1542.2	2320.0	3180.7	4112.4	5106.6	6157.0
$\mathscr{J}$	0.0110	0.0146	0.0178	0.0207	0.0234	0.0259	0.0283	0.0306
Ce^{134}								
$E_{expt}{}^{f}$	409.2	1048.6	1862.0	2809.0				
E	407.0	1060.5	1866.1	2786.5	3801.2	4896.7	6063.4	7294.2
$\mathscr{J}$	0.0090	0.0122	0.0150	0.0175	0.0199	0.0221	0.0242	0.0262
Ce^{136}								
$E_{expt}{}^{f}$	552.0	1313.6	2213.0					
E	552.2	1313.0	2215.1	3226.0	4327.3	5506.5	6754.8	8065.6
$\mathscr{J}$	0.0074	0.0107	0.0135	0.0161	0.0184	0.0206	0.0226	0.0246
Sm^{150}								
$E_{expt}{}^{g}$	330±3	775±8	1270±10					
E	331.1	767.0	1279.0	1849.9	2470.1	3132.7	3833.2	4567.8
$\mathscr{J}$	0.0128	0.0188	0.0239	0.0285	0.0327	0.0366	0.0404	0.0440
Sm^{152}								
$E_{expt}{}^{e,g}$	121.78±0.05	366.4±0.3	712±3	1122±10	1615±15			
E	121.0	369.9	712.3	1127.3	1601.8	2127.2	2697.2	3307.0
$\mathscr{J}$	0.0260	0.0300	0.0341	0.0380	0.0419	0.0455	0.0491	0.0525
Sm^{154}								
$E_{expt}{}^{e}$	81.99±0.05	267±1	545±5	927±20				
E	81.5	267.7	550.4	920.3	1368.3	1886.5	2468.2	3107.7
$\mathscr{J}$	0.0370	0.0381	0.0397	0.0414	0.0433	0.0454	0.0474	0.0495
Gd^{152}								
$E_{expt}{}^{a,g}$	344.24±0.05	755.6±0.5	1285±10					
E	341.9	769.7	1267.2	1819.3	2417.1	3054.4	3727.1	4431.6
$\mathscr{J}$	0.0130	0.0193	0.0247	0.0295	0.0339	0.0381	0.0421	0.0458

TABLE I (*Continued*)

I	2	4	6	8	10	12	14	16
Gd^{154}								
E_{expt}[a,g]	123.07±0.05	371.2±0.2	718.1±1	1146±10	1644±15	(2189)		
E	122.0	374.4	722.8	1146.0	1630.7	2167.8	2750.9	3375.1
$\mathcal{J}$	0.0257	0.0295	0.0334	0.0373	0.0410	0.0445	0.0480	0.0513
Gd^{156}								
E_{expt}[a,g]	88.967±0.005	288.16±0.05	584.5±0.5	966±5	(1411)			
E	88.8	288.4	585.0	965.2	1417.9	1934.2	2506.9	3130.7
$\mathcal{J}$	0.0342	0.0359	0.0382	0.0406	0.0432	0.0458	0.0484	0.0509
Gd^{158}								
E_{expt}[e]	79.51±0.01	261.45±0.05	539.03±0.05	898.2±0.5				
E	79.6	261.4	537.8	899.5	1338.0	1845.4	2415.3	3042.1
$\mathcal{J}$	0.0379	0.0390	0.0405	0.0423	0.0443	0.0463	0.0484	0.0505
Gd^{160}								
E_{expt}[e]	75.3±0.5	247±2	509±5	863±10				
E	75.1	247.5	511.5	860.0	1285.7	1781.8	2342.2	2961.7
$\mathcal{J}$	0.0401	0.0410	0.0423	0.0438	0.0454	0.0472	0.0491	0.0509
Dy^{154}								
E_{expt}[h]	334.7	747.0	1224.4	1748.2	2305.5			
E	333.7	744.8	1221.5	1749.7	2321.1	2929.9	3572.1	4244.6
$\mathcal{J}$	0.0135	0.0201	0.0258	0.0309	0.0355	0.0399	0.0441	0.0481
Dy^{156}								
E_{expt}[i]	138±3	403±6	766±10	1212±15				
E	137.1	407.3	769.3	1201.3	1690.3	2228.1	2808.5	3427.1
$\mathcal{J}$	0.0235	0.0280	0.0325	0.0368	0.0408	0.0446	0.0483	0.0518
Dy^{158}								
E_{expt}[i]	99±1	317±3	633±6	1037±10	1512±15	(2037)		
E	98.8	317.0	635.3	1036.9	1509.2	2042.7	2630.3	3266.4
$\mathcal{J}$	0.0309	0.0331	0.0358	0.0387	0.0416	0.0445	0.0473	0.0501
Dy^{160}								
E_{expt}[i]	86.7±0.1	284±1	582±2	972±5	1442±10			
E	86.7	284.0	582.6	971.7	1441.5	1983.4	2590.2	3256.0
$\mathcal{J}$	0.0349	0.0360	0.0376	0.0394	0.0414	0.0434	0.0455	0.0476
Dy^{162}								
E_{expt}[i]	81±0.3	266±1	548±3	923±5				
E	80.9	266.2	549.2	921.5	1374.8	1901.6	2495.3	3150.2
$\mathcal{J}$	0.0373	0.0382	0.0395	0.0410	0.0427	0.0445	0.0464	0.0483
Dy^{164}								
E_{expt}[e]	73.39±0.05	242.2±0.1	501.3±0.5	839±5				
E	73.5	242.1	500.1	840.3	1255.4	1738.7	2284.2	2886.8
$\mathcal{J}$	0.0410	0.0419	0.0433	0.0448	0.0466	0.0485	0.0504	0.0524

TABLE I (*Continued*)

I	2	4	6	8	10	12	14	16
Er^{156}								
$E_{expt}{}^{j}$	344.4±1	797.3±2	1340.5±4	1958.7±6				
E	343.3	802.4	1343.2	1947.3	2604.1	3306.4	4049.2	4828.4
σ	0.0123	0.0179	0.0226	0.0269	0.0309	0.0346	0.0381	0.0414
Er^{158}								
$E_{expt}{}^{j}$	192.7±1	528.4±2	972.2±3	1496.0±4	2075.7±7	2684.4±10		
E	191.3	535.1	975.8	1489.5	2062.7	2686.6	3355.2	4063.8
σ	0.0177	0.0226	0.0271	0.0312	0.0350	0.0386	0.0421	0.0454
Er^{160}								
$E_{expt}{}^{j}$	126.2±1	390.5±2	766.8±3	1231.4±4	1763.5±6	2342.9±8		
E	125.8	392.5	767.1	1227.4	1758.4	2350.0	2994.9	3687.3
σ	0.0247	0.0277	0.0309	0.0342	0.0373	0.0404	0.0433	0.0462
Er^{162}								
$E_{expt}{}^{g}$	101±1	327±3	662±7	1090±10	1595±15			
E	101.0	327.1	661.7	1089.1	1596.4	2173.5	2812.7	3507.7
σ	0.0301	0.0318	0.0339	0.0362	0.0386	0.0410	0.0434	0.0457
Er^{164}								
$E_{expt}{}^{g}$	91.0±1	298±3	608±6	1014±10	1512±15			
E	90.9	297.6	610.0	1016.7	1507.1	2072.3	2704.7	3398.2
σ	0.0333	0.0344	0.0359	0.0377	0.0397	0.0416	0.0437	0.0457
Er^{166}								
$E_{expt}{}^{e,g}$	80.6±0.05	264.9±0.2	545±1	910±5	(1340)			
E	80.6	264.8	544.6	910.6	1354.2	1867.3	2443.5	3077.0
σ	0.0374	0.0385	0.0400	0.0418	0.0438	0.0458	0.0479	0.0499
Er^{168}								
$E_{expt}{}^{a}$	79.8±5	264±0.5	549±0.5					
E	79.8	264.1	548.9	928.9	1398.0	1950.2	2579.6	3281.1
σ	0.0377	0.0382	0.0390	0.0399	0.0410	0.0422	0.0435	0.0448
Er^{170}								
$E_{expt}{}^{e}$	79±0.5	261±2	542±3					
E	79.0	261.1	541.9	915.3	1374.8	1914.0	2526.9	3208.0
σ	0.0381	0.0387	0.0396	0.0407	0.0419	0.0433	0.0447	0.0462
Yb^{158}								
$E_{expt}{}^{j}$	357.9±2	833.9±4	1382.2±6					
E	358.3	830.8	1385.9	2005.1	2677.6	3396.3	4156.1	4952.9
σ	0.0119	0.0174	0.0221	0.0263	0.0301	0.0338	0.0372	0.0405
Yb^{160}								
$E_{expt}{}^{j}$	243.0±1	638.3±3	1147.1±5	1735.8±7				
E	241.8	644.9	1147.6	1725.4	2364.6	3056.4	3794.6	4574.3
σ	0.0147	0.0196	0.0239	0.0279	0.0315	0.0349	0.0382	0.0413

Table I (*Continued*)

I	2	4	6	8	10	12	14	16
Yb^{162}								
E_{expt}[j]	166.5±1	486.7±2	922.9±4	1444.1±6	2013.5±8			
E	166.0	490.2	922.3	1436.6	2017.8	2656.0	3344.3	4077.4
$\mathcal{I}$	0.0195	0.0234	0.0273	0.0309	0.0344	0.0376	0.0408	0.0438
Yb^{164}								
E_{expt}[k]	122.5±0.5	384±1	758±1	1219±4	1748±5	(2322)	(2928)	
E	122.4	384.8	757.0	1217.2	1750.5	2346.4	2997.5	3697.9
$\mathcal{I}$	0.0252	0.0280	0.0310	0.0341	0.0371	0.0400	0.0428	0.0456
Yb^{166}								
E_{expt}[k]	101.8±0.4	329.7±1	667.1±2	1097.0±4	1604±5	2172±6	(2774.4)	(3402.2)
E	101.9	329.6	666.4	1096.1	1605.8	2185.3	2826.9	3524.2
$\mathcal{I}$	0.0298	0.0316	0.0338	0.0361	0.0386	0.0410	0.0433	0.0456
Yb^{168}								
E_{expt}[g]	87±1	284±3	582±6	967±10	1427±15	(1932)		
E	87.0	284.3	581.2	966.1	1428.7	1960.1	2553.3	3202.5
$\mathcal{I}$	0.0348	0.0361	0.0379	0.0399	0.0421	0.0443	0.0466	0.0488
Yb^{170}								
E_{expt}[g]	84.2±0.1	277.7±1	572±3	962±5	1439±8	(1986)		
E	84.2	277.4	572.9	962.4	1437.7	1990.9	2615.3	3304.9
$\mathcal{I}$	0.0358	0.0366	0.0378	0.0392	0.0407	0.0424	0.0441	0.0458
Yb^{172}								
E_{expt}[g]	78.7±0.5	260.3±1	540.0±3	910±5	1352±8			
E	78.9	260.3	538.6	906.6	1357.0	1882.9	2477.8	3136.4
$\mathcal{I}$	0.0382	0.0389	0.0400	0.0414	0.0429	0.0445	0.0462	0.0479
Yb^{174}								
E_{expt}[e]	76.5±0.5	252±3	527±5	892±8				
E	76.3	252.9	526.3	891.9	1344.4	1878.3	2488.4	3169.8
$\mathcal{I}$	0.0394	0.0399	0.0406	0.0414	0.0425	0.0436	0.0448	0.0461
Yb^{176}								
E_{expt}[e]	82.1±0.5	270±3	564±5	947±10				
E	82.0	271.0	561.9	948.2	1422.9	1979.1	2610.6	3311.6
$\mathcal{I}$	0.0367	0.0373	0.0382	0.0394	0.0406	0.0420	0.0434	0.0449
Hf^{166}								
E_{expt}[k]	158.7±0.4	470.7±1.5	897.6±3	1407.0±4	1971±6	2565±10	(3178)	
E	158.9	472.7	893.5	1395.9	1965.0	2590.9	3266.6	3986.8
$\mathcal{I}$	0.0202	0.0241	0.0279	0.0316	0.0350	0.0383	0.0415	0.0445
Hf^{168}								
E_{expt}[k]	123.9±0.4	385±1	756.1±3	1212±4	1734±5	2304±10	(2910)	
E	123.8	386.2	755	1208.0	1730.7	2313.0	2947.8	3629.3
$\mathcal{I}$	0.0251	0.0281	0.0314	0.0347	0.0379	0.0410	0.0440	0.0469

TABLE I (*Continued*)

I	2	4	6	8	10	12	14	16
Hf^{170}								
$E_{\mathrm{expt}}{}^{k}$	100.0±0.3	320.6±1	641.1±3	1041.0±4	1503±6	2013±8	2564±10	3147±20
E	101.0	320.7	636.7	1031.0	1491.1	2007.9	2574.5	3185.7
g	0.0304	0.0331	0.0363	0.0396	0.0429	0.0460	0.0492	0.0522
Hf^{172}								
$E_{\mathrm{expt}}{}^{k}$	94.5±0.3	307.9±1	627±3	1036±4	1519±6	2063±8	2651±10	(3273)
E	95.0	308.1	624.7	1030.2	1512.5	2062.2	2671.9	3335.6
g	0.0320	0.0336	0.0358	0.0381	0.0406	0.0430	0.0455	0.0479
Hf^{174}								
$E_{\mathrm{expt}}{}^{g,l}$	90.9	298.0	609.0	1010.0	1502.0			
E	91.0	297.5	608.8	1013.1	1499.5	2059.0	2684.1	3368.7
g	0.0333	0.0345	0.0361	0.0380	0.0401	0.0421	0.0442	0.0463
Hf^{176}								
$E_{\mathrm{expt}}{}^{m}$	88.3±0.3	290.0±0.5	596.6±0.6	998.0±0.8				
E	88.1	289.6	596.2	998.3	1486.5	2052.3	2688.4	3388.7
g	0.0342	0.0352	0.0365	0.0380	0.0397	0.0415	0.0433	0.0451
Hf^{178}								
$E_{\mathrm{expt}}{}^{a}$	93.2±0.1	306.8±0.2	632.5±0.5	1059±3				
E	93.2	306.7	632.1	1059.5	1579.1	2182.0	2860.7	3608.7
g	0.0323	0.0332	0.0344	0.0358	0.0373	0.0389	0.0406	0.0422
Hf^{180}								
$E_{\mathrm{expt}}{}^{a}$	93.33±0.05	308.6±0.2	641.1±0.3	1084.9±0.5				
E	93.3	308.7	641.3	1084.7	1631.6	2274.8	3007.4	3823.2
g	0.0322	0.0327	0.0334	0.0342	0.0352	0.0363	0.0374	0.0386
W^{172}								
$E_{\mathrm{expt}}{}^{k}$	122.9±0.4	376.9±1	727.2±3	1147±4	1616±6	2129±8	2677±10	(3253)
E	123.8	376.1	720.9	1137.1	1611.8	2136.4	2704.8	3312.2
g	0.0255	0.0297	0.0339	0.0380	0.0419	0.0456	0.0492	0.0527
W^{174}								
$E_{\mathrm{expt}}{}^{k}$	111.9±0.3	355±1	704.2±3	1137±4	1635±6	2186±8	(2780)	
E	112.2	354.9	701.8	1132.9	1634.4	2196.4	2811.6	3474.4
g	0.0274	0.0301	0.0332	0.0363	0.0394	0.0424	0.0453	0.0481
W^{176}								
$E_{\mathrm{expt}}{}^{k}$	108.7±0.3	348.5±1	699.4±3	1140±4	1648±6	2206±8	(2801)	(3425)
E	109.1	348.7	696.4	1133.2	1645.4	2222.7	2857.4	3543.6
g	0.0281	0.0303	0.0329	0.0357	0.0384	0.0412	0.0439	0.0464
W^{178}								
$E_{\mathrm{expt}}{}^{n}$	104±5	342±7	697±10	1152±15	1679±20	2264±25	2894±30	
E	105.4	341.4	690.7	1136.9	1666.5	2269.1	2936.5	3662.3
g	0.0288	0.0304	0.0325	0.0347	0.0370	0.0393	0.0415	0.0438

TABLE I (*Continued*)

I	2	4	6	8	10	12	14	16
W^{180}								
$E_{expt}{}^{n}$	102±5	336±7	690±10	1147±15	1667±20	2252±25		
E	103.1	335.7	683.5	1131.5	1667	2279.8	2961.4	3705.2
$\mathcal{I}$	0.0294	0.0307	0.0325	0.0344	0.0365	0.0385	0.0406	0.0427
W^{182}								
$E_{expt}{}^{a,n}$	100.1±0.05	329.4±0.05	680.4±0.5	1138±10	(1646)			
E	100.0	329.2	678.9	1138.0	1698.7	2349.1	3081.9	3890.0
$\mathcal{I}$	0.0301	0.0309	0.0319	0.0332	0.0346	0.0361	0.0376	0.0391
W^{184}								
$E_{expt}{}^{a}$	111.2	364.0	748.2					
E	111.1	364.4	747.8	1248.0	1852.3	2549.8	3331.3	4189.1
$\mathcal{I}$	0.0272	0.0281	0.0293	0.0307	0.0322	0.0337	0.0353	0.0369
W^{186}								
$E_{expt}{}^{a}$	122.5	399.0	818.0					
E	122.4	399.8	817.2	1358.3	2008.3	2755.1	3588.5	4500.6
$\mathcal{I}$	0.0247	0.0257	0.0270	0.0284	0.0300	0.0316	0.0332	0.0348
Os^{178}								
$E_{expt}{}^{o}$	131.6±0.3	397.7±1	760.8±2	1193.7±3	1681.7±4	2218.5±5		
E	131.9	397.5	757.8	1190.8	1683.3	2226.5	2814.1	3441.5
$\mathcal{I}$	0.0241	0.0283	0.0325	0.0366	0.0404	0.0441	0.0477	0.0511
Os^{180}								
$E_{expt}{}^{o}$	132.2±0.3	408.5±1	795.1±2	1257.3±3	1767.5±4	2308.5±6	(2874.9)	
E	133.4	407.8	785.5	1243.2	1766.6	2346.1	2974.8	3647.4
$\mathcal{I}$	0.0236	0.0272	0.0309	0.0345	0.0380	0.0413	0.0445	0.0476
Os^{182}								
$E_{expt}{}^{o}$	126.9±0.3	400.2±1	793.9±2	1276.9±3	1809.6±5			
E	127.3	400.5	788.7	1268.9	1825.8	2448.5	3129.0	3861.2
$\mathcal{I}$	0.0243	0.0268	0.0297	0.0326	0.0355	0.0383	0.0410	0.0436
Os^{184}								
$E_{expt}{}^{p}$	119.8±0.3	383.6±0.4	773.9±0.6	1274.6±0.7	(1871.2)			
E	119.4	385.0	775.4	1271.1	1856.8	2520.8	3254.2	4049.8
$\mathcal{I}$	0.0225	0.0271	0.0291	0.0313	0.0335	0.0357	0.0379	0.0400
Os^{186}								
$E_{expt}{}^{p}$	137.2±0.5	433.9±0.1	868.7±0.1	1420.5±0.3	(2068.1)			
E	136.6	436.3	870.6	1415.8	2054.5	2774.0	3564.8	4419.5
$\mathcal{I}$	0.0224	0.0242	0.0264	0.0286	0.0308	0.0330	0.0352	0.0372
Os^{188}								
$E_{expt}{}^{p}$	155.0±0.1	477.9±0.1	939.8±0.3	1513.6±0.5	(2169.5)			
E	154.3	481.4	941.5	1506.9	2159.6	2886.9	3679.8	4531.3
$\mathcal{I}$	0.0201	0.0225	0.0251	0.0278	0.0303	0.0328	0.0352	0.0375
Os^{190}								
$E_{expt}{}^{q}$	186.7±0.1	547.8±0.1	1050±5	1662±10				
E	185.3	554.6	1052.4	1648.5	2325.0	3069.8	3874.8	4733.4
$\mathcal{I}$	0.0172	0.0204	0.0236	0.0266	0.0295	0.0322	0.0348	0.0373

TABLE I (*Continued*)

I	2	4	6	8	10	12	14	16
Pt^{182}								
E_{expt}[o]	153.7±0.4	416.2±1	771.4±2	1202.4±3	(1695.4)	(2238.4)		
E	152.0	425.1	775.2	1183.3	1638.6	2134.2	2665.2	3228.1
σ	0.0223	0.0285	0.0341	0.0392	0.0441	0.0486	0.0529	0.0571
Pt^{184}								
E_{expt}[o]	162.1±0.4	434.8±1	797.3±2	1228.9±3	1704.7±4	(2201.3)	(2723)	(3726)
E	160.2	443.1	803.4	1221.8	1687.6	2194.0	2736.0	3309.9
σ	0.0214	0.0276	0.0332	0.0383	0.0431	0.0476	0.0519	0.0560
Pt^{186}								
E_{expt}[o]	191.1±0.6	489.6±1.5	876.8±2	1341.1±3	1855.7±5	(2407)		
E	188.4	500.2	888.1	1333.4	1825.7	2358.3	2926.3	3526.1
σ	0.0190	0.0254	0.0310	0.0361	0.0409	0.0454	0.0496	0.0537
Pt^{188}								
E_{expt}[o]	265.9±0.6	671.3±2	1184.6±3	(1782)	(2436)			
E	265.2	676.4	1178.2	1748.8	2375.8	3051.3	3769.7	4526.6
σ	0.0141	0.0195	0.0241	0.0283	0.0322	0.0358	0.0393	0.0426
Pt^{190}								
E_{expt}[n]	292±5	733±10	1283±15	1903±20	2636±25			
E	290.1	740.0	1288.9	1913.0	2598.9	3337.9	4123.7	4951.7
σ	0.0129	0.0178	0.0220	0.0259	0.0294	0.0327	0.0359	0.0389
Pt^{192}								
E_{expt}[n]	317±1	785±1	1388±10	2063±20				
E	315.0	797.2	1383.7	2049.3	2780.1	3566.9	4403.2	5283.9
σ	0.0120	0.0166	0.0207	0.0243	0.0276	0.0307	0.0337	0.0366
Pt^{194}								
E_{expt}[r]	328.5±1	811.1±2	1411.6±3	2099.4±5				
E	327.1	818.6	1413.2	2086.5	2824.5	3618.2	4461.2	5348.5
σ	0.0117	0.0164	0.0204	0.0240	0.0274	0.0305	0.0335	0.0363
Th^{228}								
E_{expt}[a]	57.5±0.1	186.6±0.2	378±1					
E	57.5	186.5	378.1	623.3	915.0	1247.4	1616.0	2017.2
σ	0.0528	0.0556	0.0591	0.0630	0.0671	0.0712	0.0752	0.0792
Th^{232}								
E_{expt}[a]	49.8±0.1	163±1	333±3	555±5	828±8			
E	49.7	162.9	333.9	556.6	825.2	1134.9	1481.4	1861.5
σ	0.0608	0.0629	0.0657	0.0689	0.0724	0.0760	0.0797	0.0833
U^{232}								
E_{expt}[a]	47.6±0.1	156.6±0.2	321±1					
E	47.6	156.3	321.2	536.7	797.4	1098.8	1436.8	1808.2
σ	0.0634	0.0653	0.0680	0.0711	0.0745	0.0780	0.0816	0.0852

TABLE I (*Continued*)

I	2	4	6	8	10	12	14	16
U^{234}								
E_{expt}[a]	43.50±0.05	143.5±0.2	296.6±3	(499)				
E	43.5	143.5	296.6	499.0	746.3	1034.7	1360.7	1721.3
$\mathcal{I}$	0.0693	0.0707	0.0728	0.0754	0.0782	0.0812	0.0843	0.0875
U^{236}								
E_{expt}[a]	45.28±0.05	148.7±0.5	312±1					
E	45.1	149.6	311.2	527.4	795.0	1110.7	1471.5	1874.3
$\mathcal{I}$	0.0666	0.0674	0.0686	0.0701	0.0718	0.0738	0.0758	0.0780
U^{238}								
E_{expt}[a]	44.7±0.1	148±1	309±2	523±3	787±5	1100±8		
E	44.7	148.2	308.4	522.5	787.6	1100.3	1457.7	1856.6
$\mathcal{I}$	0.0672	0.0680	0.0692	0.0708	0.0725	0.0745	0.0766	0.0787
Pu^{238}								
E_{expt}[a]	44.11±0.05	146.0±0.5	303.6±1	514±5				
E	44.1	146.0	303.6	514.0	773.9	1080.0	1429.3	1818.7
$\mathcal{I}$	0.0682	0.0691	0.0704	0.0721	0.0740	0.0761	0.0784	0.0807
Pu^{240}								
E_{expt}[a]	42.88±0.05	141.7±0.5	296±5					
E	42.8	142.0	295.7	501.5	756.5	1057.8	1402.5	1787.8
$\mathcal{I}$	0.0702	0.0710	0.0721	0.0736	0.0753	0.0773	0.0793	0.0815
Cm^{242}								
E_{expt}[a]	42.2±0.1	139±3	285±5					
E	42.2	138.7	285.3	477.0	709.3	978.0	1279.7	1611.4
$\mathcal{I}$	0.0715	0.0736	0.0765	0.0799	0.0836	0.0875	0.0914	0.0954
Cm^{244}								
E_{expt}[a]	42.9±0.1	142.3±0.5	296±5	502±10				
E	42.9	142.2	296.1	502.0	757.0	1058.2	1402.5	1787.4
$\mathcal{I}$	0.0701	0.0709	0.0721	0.0736	0.0754	0.0773	0.0794	0.0816
Cm^{248}								
E_{expt}[a]	43.4±0.1	143.6±0.5	300±10					
E	43.4	143.8	299.8	509.1	769.1	1077.1	1430.2	1826.0
$\mathcal{I}$	0.0693	0.0700	0.0710	0.0723	0.0738	0.0755	0.0773	0.0793

[a] Reference 37.
[b] J. A. Moragues, P. Reyes-Suter, and T. Suter, Nucl. Phys. **A99**, 652 (1967).
[c] Reference 24.
[d] Reference 19. The value for E_{expt} (Xe^{130}; $I=2$) is a weighted average obtained from the recent literature.
[e] *Nuclear Data Sheets*, compiled by K. Way *et al.* (Printing and Publishing Office, National Academy of Sciences–National Research Council, Washington, D.C. 20025), NRC 1963–4; Ref. 36.
[f] Reference 39.
[g] Reference 20.
[h] Reference 38.
[i] Reference 17.
[j] Reference 26.
[k] Reference 22.
[l] S. Graetzer, G. B. Hagemann, K. A. Hagemann, and B. Elbek, Nucl. Phys. **76**, 1 (1966).
[m] A. W. Sunyar (private communication).
[n] Reference 18.
[o] Reference 23.
[p] Reference 25.
[q] G. Scharff-Goldhaber, D. E. Alburger, G. Harbottle, and M. McKeown, Phys. Rev. **111**, 913 (1958).
[r] Reference 42.

TABLE II. Values of the parameters $\mathcal{J}_0$ and C obtained from the least-squares fit and the softness σ derived from them.

Nucleus	$\mathcal{J}_0$ (keV^{-1})	C (10^6 keV^3)	$\sigma=1/2C\mathcal{J}_0^3$
Pd^{108}	0.0029	5.40	3.92
Cd^{110}	0.0007	12.12	110
Xe^{120}	0.0056	3.36	0.971
Xe^{122}	0.0058	4.24	0.585
Xe^{124}	0.0053	4.92	0.678
Xe^{126}	0.0041	4.92	1.54
Xe^{128}	0.0020	4.56	14.1
Xe^{130}	0.00001	5.08	106×10^6
Ba^{124}	0.0115	4.76	0.070
Ba^{126}	0.0103	6.16	0.074
Ce^{128}	0.0133	5.44	0.038
Ce^{130}	0.0103	5.80	0.079
Ce^{132}	0.0069	6.08	0.250
Ce^{134}	0.0050	9.32	0.416
Ce^{136}	0.0020	10.00	6.79
Sm^{150}	0.0021	1.68	33.5
Sm^{152}	0.0234	1.68	0.229
Sm^{154}	0.0365	4.36	0.0024
Gd^{152}	0.0005	1.44	2530
Gd^{154}	0.0233	1.84	0.021
Gd^{156}	0.0333	2.96	0.0045
Gd^{158}	0.0374	4.08	0.0023
Gd^{160}	0.0397	4.64	0.0017
Dy^{154}	0.00002	1.24	437×10^6
Dy^{156}	0.0201	1.60	0.039
Dy^{158}	0.0298	2.64	0.0071
Dy^{160}	0.0343	4.56	0.0027
Dy^{162}	0.0369	5.12	0.0019
Dy^{164}	0.0406	4.20	0.0018
Er^{156}	0.0024	2.04	17.8
Er^{158}	0.0131	2.04	0.109
Er^{160}	0.0229	2.72	0.015
Er^{162}	0.0293	3.92	0.0051
Er^{164}	0.0327	5.08	0.0028
Er^{166}	0.0369	4.16	0.0024
Er^{168}	0.0375	9.08	0.0010
Er^{170}	0.0378	7.56	0.0012
Yb^{158}	0.0020	2.16	31.3
Yb^{160}	0.0092	2.48	0.259
Yb^{162}	0.0164	2.60	0.043
Yb^{164}	0.0237	3.00	0.013
Yb^{166}	0.0289	3.92	0.0052
Yb^{168}	0.0342	3.88	0.0032
Yb^{170}	0.0354	6.24	0.0018
Yb^{172}	0.0379	4.68	0.0016
Yb^{174}	0.0392	9.28	0.0009
Yb^{176}	0.0364	7.84	0.0013
Hf^{166}	0.0173	2.52	0.038
Hf^{168}	0.0233	2.60	0.015
Hf^{170}	0.0289	2.12	0.0096
Hf^{172}	0.0312	3.52	0.0047
Hf^{174}	0.0327	4.64	0.0031
Hf^{176}	0.0338	5.88	0.0022
Hf^{178}	0.0320	7.40	0.0021
Hf^{180}	0.0321	13.8	0.0011
W^{172}	0.0227	1.64	0.026
W^{174}	0.0260	2.64	0.011
W^{176}	0.0269	3.24	0.0080
W^{178}	0.0280	4.48	0.0050
W^{180}	0.0288	5.32	0.0039
W^{182}	0.0298	10.24	0.0018
W^{184}	0.0268	9.76	0.0026
W^{186}	0.0243	10.80	0.0033
Os^{178}	0.0212	1.76	0.030
Os^{180}	0.0213	2.28	0.023
Os^{182}	0.0228	3.40	0.012
Os^{184}	0.0247	5.56	0.0060
Os^{186}	0.0215	6.16	0.0082
Os^{188}	0.0187	5.12	0.015
Os^{190}	0.0150	4.36	0.034
Pt^{182}	0.0165	1.04	0.109
Pt^{184}	0.0153	1.08	0.133
Pt^{186}	0.0116	1.12	0.284
Pt^{188}	0.0071	2.12	0.675
Pt^{190}	0.0064	2.76	0.676
Pt^{192}	0.0057	3.28	0.816
Pt^{194}	0.0052	3.32	1.10
Th^{228}	0.0515	0.76	0.0047
Th^{232}	0.0598	0.84	0.0028
U^{232}	0.0625	0.84	0.0025
U^{234}	0.0686	0.92	0.0017
U^{236}	0.0663	1.92	0.00090
U^{238}	0.0669	1.84	0.00091
Pu^{238}	0.0678	1.60	0.00099
Pu^{240}	0.0698	1.76	0.00084
Cm^{242}	0.0705	0.60	0.0024
Cm^{244}	0.0697	1.72	0.00086
Cm^{248}	0.0690	2.12	0.00072

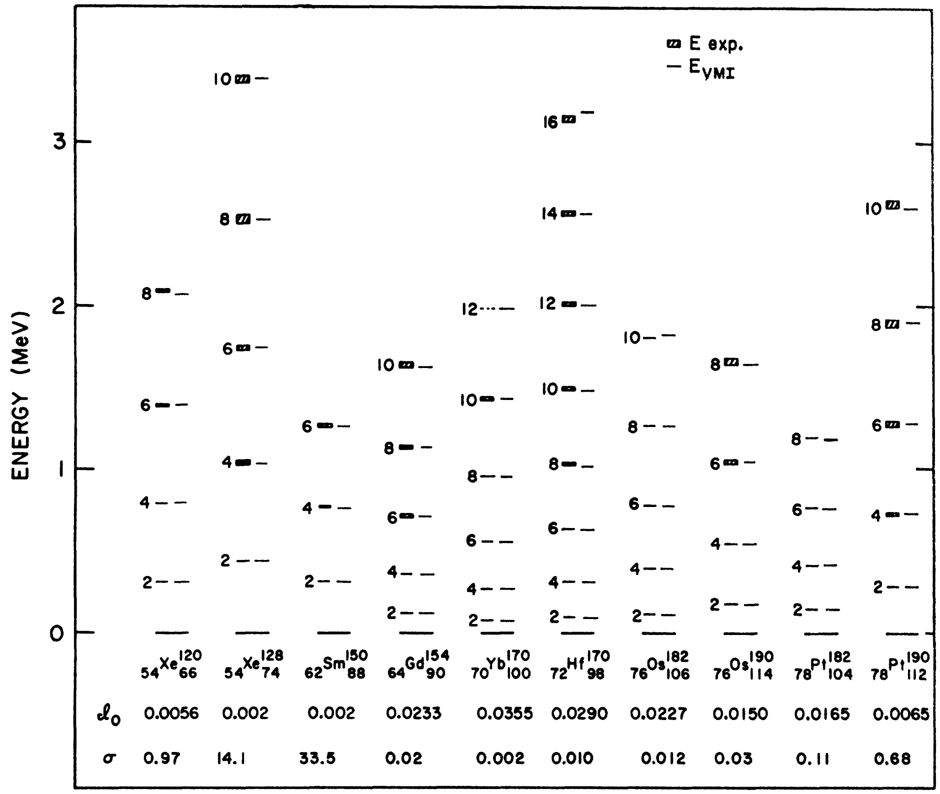

FIG. 6. Experimental and calculated ground-state bands of some even-even nuclei. For each nucleus, the experimental energies are shown on the left and the calculated energies on the right. The values of the parameters $\mathcal{J}_0$ and σ corresponding to each nucleus are listed at the bottom of the figure.

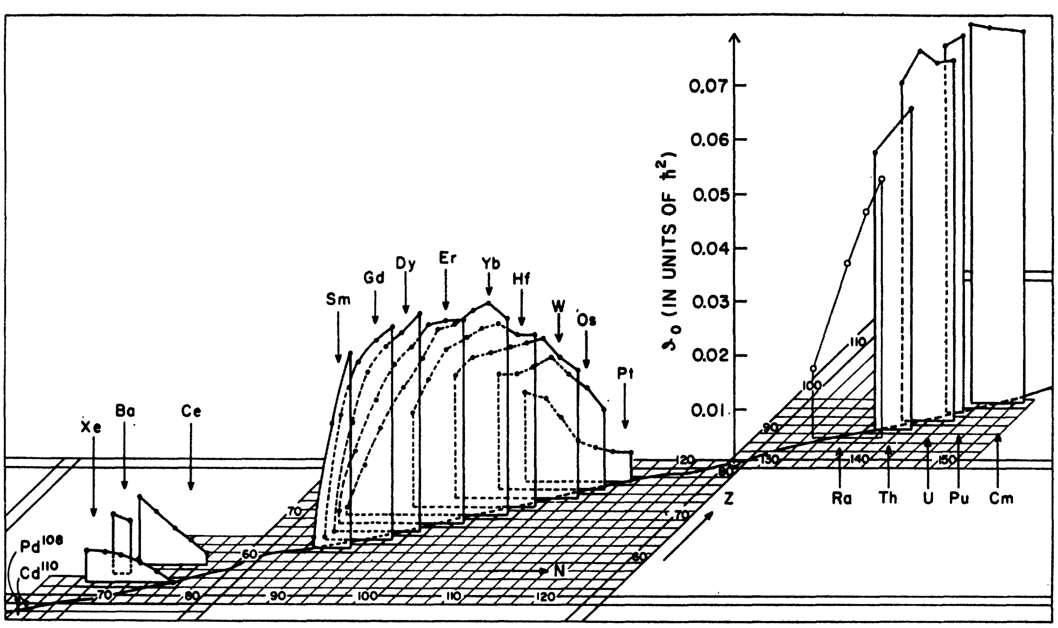

FIG. 7. Calculated ground-state moment of inertia $\mathcal{J}_0$ of even-even nuclei as a function of Z and N. Only those nuclei (Table I) with at least three known levels (2+, 4+, 6+) of the band are included, with the exception of the Ra isotopes, for which only the 2+ and 4+ states are known. The latter are included to show the transition to the well-deformed heavy elements.

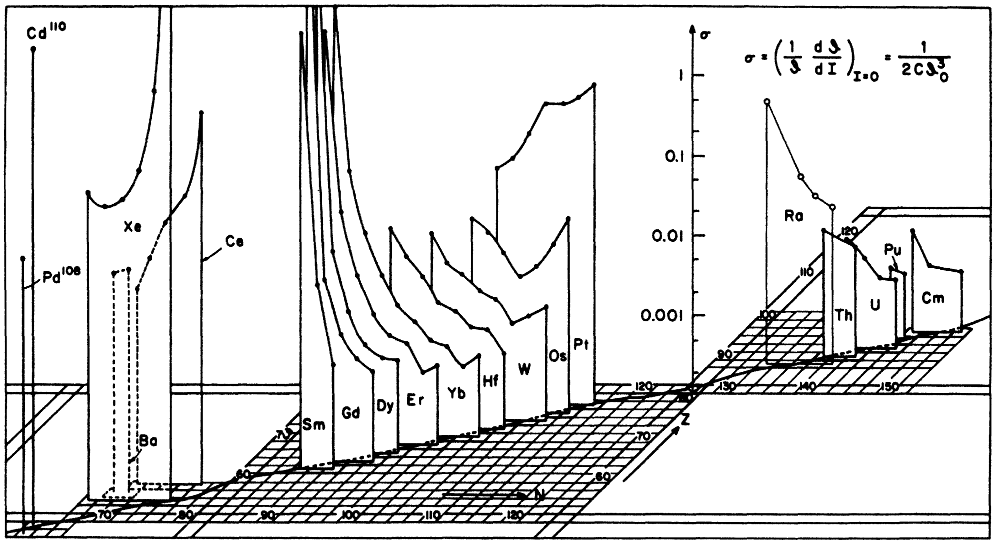

FIG. 8. Calculated softness parameter σ of even-even nuclei as a function of Z and N (on a logarithmic scale). Only those nuclei (Table I) with at least three known levels (2+, 4+, 6+) of the band are included, with the exception of the Ra isotopes, for which only the 2+ and 4+ states are known. The latter are included to show the transition to the well-deformed heavy elements.

from the almost-spherical to the well-deformed nuclei between 88 and 90 neutrons. However, as Stephens, Ward, and Newton,[26] who used Ar^{40} ions to populate ground-state bands in very neutron-deficient $_{66}Dy$, $_{68}Er$, and $_{70}Yb$ nuclei, have pointed out, the 88–90 neutron "discontinuity" is smeared out as the proton number increases beyond $Z=66$. This fact is reflected in Figs. 7 and 8. It is seen that for $Z>68$ (Er isotopes and beyond) the transition becomes more gradual as had been found to be characteristic of the Os isotopes.[13,14]

In the rare-earth region the softness parameter σ decreases and $\mathcal{J}_0$ increases as the stability line is approached; e.g., for the radioactive nucleus Dy^{154} the model gives an extremely small moment of inertia for the ground state, $\mathcal{J}_0 = 2\times10^{-5}$ (i.e., $\sim$2000 times smaller than the $\mathcal{J}_0$ value for the stable nucleus Dy^{164}), while the moment of inertia of the 2^+ state is approximately 1.4×10^{-2}, that is, 700 times larger than $\mathcal{J}_0$. Correspondingly, the softness parameter of Dy^{154} is $\sigma=4.4\times10^8$ as compared with $\sigma=0.0018$ for Dy^{164} (Fig. 8). A graphic description for the transitional properties of the Os nuclei, as mentioned in the Introduction, is displayed at the end of the rare-earth region. Here $\mathcal{J}_0$ and σ show a unique behavior: $\mathcal{J}_0$ increases to a maximum at $Os_{108}{}^{184}$ and then decreases fairly steeply, while σ decreases steeply to Os^{184} and then increases just as rapidly to Os^{190}. In this connection it is noteworthy that the one neutron binding energy of the 108th neutron reverses its trend and decreases for Os^{184}.[40] The parameters obtained for the Pt isotopes are perhaps even more interesting. Here $\mathcal{J}_0$ decreases steeply to $Pt_{110}{}^{188}$ and from there on only very slowly, while σ increases rapidly to the same nucleus and from there to Pt^{198} very gradually. Thus, even for the heaviest Pt isotopes, for which the parameters are known (Pt^{190}–Pt^{194}), the moments of inertia retain values appreciably higher than those of the $N=88$ nuclei, and the softness parameters level off. As mentioned in the Introduction, these Pt isotopes display a near-harmonic level pattern which is usually interpreted by the spherical model. In view of the rotational features emerging here, they may be called pseudospherical.[41–43] Finally, Figs. 7 and

[40] N. B. Gove and M. Yamada, Nucl. Data **A4**, 237 (1968).

TABLE III. Parameters of $K=2$ bands of even-even nuclei and ground-state (GS) bands of odd-odd nuclei compared with those of ground-state bands of appropriate even-even nuclei.

Nucleus		$\mathcal{J}_0$	σ
$_{68}Er^{166}$	GS	0.0369	0.0024
	$K=2$	0.0402	0.0021
$_{76}Os^{186}$	GS	0.0215	0.0082
	$K=2$	0.0176	0.037
$_{67}Ho^{164}$		0.0539	0.000001
$_{66}Dy^{163}$		0.0369	0.0019
$_{77}Ir^{194}$		0.0200	0.071
$_{76}Os^{192}$		0.0124	0.091

[41] It is of interest to note that in Pt^{194} a two-quasiparticle state is found below the 6+ state of the ground-state band (Ref. 42). This fact may be related to the unique behavior of the moment of inertia of the neutron-rich even-even Pt nuclei.

[42] A. W. Sunyar, G. Scharff-Goldhaber, and M. McKeown, Phys. Rev. Letters **21**, 237 (1968).

[43] See also the discussion of Pt^{194} in K. Kumar and M. Baranger, Nucl. Phys. **A110**, 529 (1968).

TABLE IV. Energies and moments of inertia of some $K=2$ bands and ground-state bands of odd-odd nuclei.

(a) $K=2$ bands								
I	2	3	4	5	6	7	8	9
Er^{166}								
$(E_I-E_2)_{expt}$[a]	0	73.4	169	289	428	588		
E_I-E_2	0	73.3	169.7	288.3	428.1	588.1	767.3	964.6
$\mathcal{J}_I$	0.0407	0.0412	0.0418	0.0425	0.0433	0.0442	0.0451	0.0461
Os^{186}								
$(E_I-E_2)_{expt}$[b]	0	142.9	302.9	507.9	723.5	984.8		
E_I-E_2	0	139.9	311.0	508.4	728.7	969.2	1228.0	1503.2
$\mathcal{J}_I$	0.0204	0.0224	0.0243	0.0263	0.0282	0.0300	0.0318	0.0336
(b) Odd-odd nuclei								
I	1	2	3	4	5	6	7	8
Ho^{164}								
$(E_I-E_1)_{expt}$[c]	0	37	93					
E_I-E_1	0	37.1	92.8	167.0	259.7	371.0	500.8	649.2
$\mathcal{J}_I$	0.0539	0.0539	0.0539	0.0539	0.0539	0.0539	0.0539	0.0539
Ir^{194}								
$(E_I-E_1)_{expt}$[d]	0	83.5	194.5					
E_I-E_1	0	83.5	194.5	327.4	478.4	645.2	825.8	1018.9
$\mathcal{J}_I$	0.0224	0.0254	0.0285	0.0316	0.0345	0.0374	0.0401	0.0427

[a] Reference 37.
[b] Reference 14.
[c] C. J. Gallagher, Jr., and V. G. Soloviev, Kgl. Danske Videnskab. Selskab, Mat.-Fys. Skrifter 2, No. 102 (1962).
[d] Deduced from Ref. 46.

8 also show the characteristics (hard and strongly deformed) of the nuclei in the heavy-element region.

Although the plots of Figs. 7 and 8 show that the values of the parameters $\mathcal{J}_0$ and σ change rather smoothly from one isotope to another, one observes that certain values appear to deviate from the general trend and that these deviations occur at certain neutron numbers: The clearest case occurs for $N=98$ nuclei. Figure 7 shows that relatively higher values of $\mathcal{J}_0$ are obtained for Dy^{164}, Er^{166}, Yb^{168}, and Hf^{170}, all $N=98$ nuclei. A similar behavior is suggested at $N=104$ and $N=108$ by the relatively high $\mathcal{J}_0$ values observed in Yb^{174} and Hf^{176}, and in Hf^{180}, W^{182}, and Os^{184}, respectively. The anomalous behavior at $N=98$ had previously been observed by Stephens, Lark, and Diamond,[21] who speculated, as a possible explanation for this effect, that the pairing correlations are reduced (implying larger moments of inertia) because of the large energy gap in the Nilsson diagram between the levels of $\frac{5}{2}^-[523]$ (98 neutrons) and $\frac{7}{2}^+[633]$. More recently, Duckworth[44] showed that breaks are also seen at $N=98$ and $N=108$ in a plot of the double-neutron separation energies as a function of the neutron number.

From Figs. 7 and 8 it is readily observed that, as a rule, large values of $\mathcal{J}_0$ correspond to small values of σ. This derives from the definition of σ [Eq. (11)] and from the relative constancy of the restoring force constant C (Table II). At neutron numbers $N=104$ and $N=108$, where relatively higher values of $\mathcal{J}_0$ are observed (Fig. 7), the values of σ are, accordingly, relatively lower. It seems very interesting, however, that this rule does not hold for $N=98$ nuclei, where the breaks in $\mathcal{J}_0$ and σ are most clearly observed. The $N=98$ nuclei display relatively high values of $\mathcal{J}_0$ and σ at the same time.

A few striking facts may be gathered from Table II: (a) The highest value of C (but not of $\mathcal{J}_0$) occurs for Hf^{180}, an almost "rigid rotor"; (b) while $\mathcal{J}_0$ changes by one or even several orders of magnitude between 88 and 90 neutrons in Sm, Gd, Dy, and Er, the parameter C remains almost unchanged, at values considerably below average; and (c) a curious coincidence is found

[44] H. E. Duckworth, Bull. Am. Phys. Soc. 12, 1055 (1967); and (private communication).

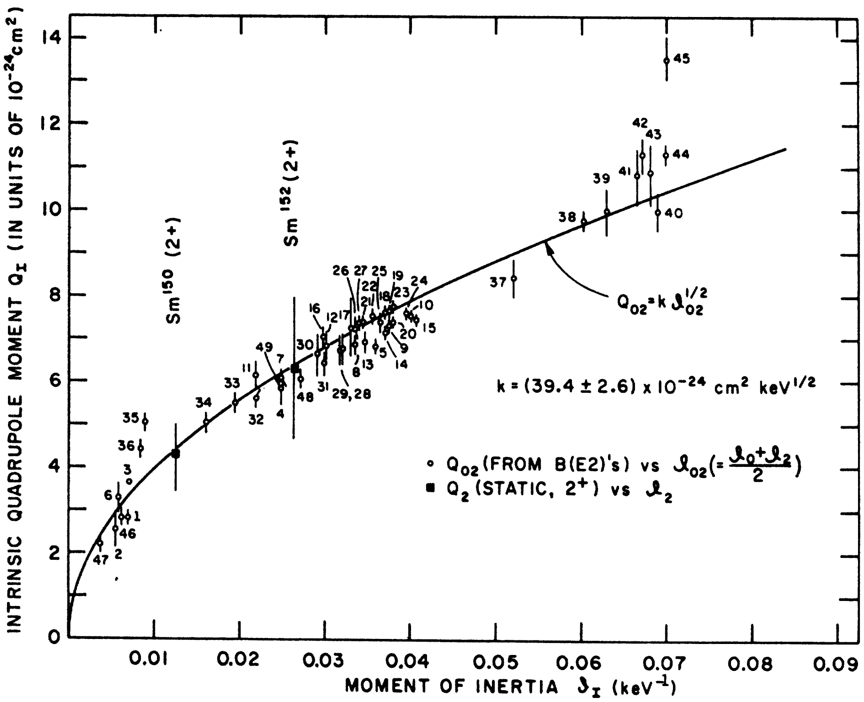

FIG. 9. Correlation between intrinsic quadrupole moments (absolute values) and moments of inertia given by the VMI model. The numbered points (open circles) refer to the transition quadrupole moments Q_{02}. They were used to determine the constant k from a least-squares fit. The coordinates of these points are given in Table V, where the numbers provide their identification. The ordinates are obtained from the $B(E2, 2\to 0)$ values (Ref. 4) and the corresponding abscissae are $\mathcal{J}_{02}=\frac{1}{2}(\mathcal{J}_0+\mathcal{J}_2)$, where $\mathcal{J}_0$ and $\mathcal{J}_2$ are taken from Tables II and I, respectively (see text). The intrinsic static quadrupole moments of the first 2+ states (Q_2) included here (solid squares), measured by the reorientation effect, are limited to Sm^{150} ("spherical") (Ref. 48) and Sm^{152} (deformed) (Ref. 49), because only for these two nuclei at least three excited states of the ground-state band are known. These $|Q_2|$ values are plotted against $\mathcal{J}_2$ (see Sec. III C).

for the nuclei Xe^{120} and Pt^{194}, which have almost identical parameters $\mathcal{J}_0$ and C.

B. Analysis of Other Rotational Bands by Means of the VMI Model

In view of the usefulness of the VMI model for the analysis of ground-state bands of even-even nuclei, one may ask oneself whether this model can also be applied to other rotational bands, and, if so, what relationship the parameters obtained in this way bear to the ground-state-band parameters.

The computer program was adapted for the analysis of other rotational bands. It was first applied to the two extensive $K=2$ (or γ-vibrational) bands in even-even nuclei, namely, in Er^{166} and Os^{186}, which both range from spin 2 to 7. The results are shown in Tables III and IV. In Table III the parameters $\mathcal{J}_0$ and σ are compared with those obtained for the ground-state bands. For Er^{166} an excellent fit to the level energies was obtained (Table IV). The parameter $\mathcal{J}_0$ for the vibrational band is somewhat larger than that for the ground-state band (as was known before). A new and interesting result was found for the softness parameter: σ_{gs} exceeds $\sigma_{K=2}$ by $\sim$10%. As expected, the fit for the $K=2$ band in Os^{186} was less good (Table IV), since in this band the even-spin levels are known to be depressed, possibly because of a repulsion by the levels of a β-vibrational band or by quasiparticle states with even spin and parity. In Os^{186} (as in the other even-even Os nuclei[14]) the parameter $\mathcal{J}_0$ for the $K=2$ band is smaller than that of the ground-state band. The softness parameter of the $K=2$ band in Os^{186}, on the other hand, is found to be appreciably larger.

Next, the rotational bands of odd-odd nuclei were analyzed. It had previously been shown[45] that the moments of inertia of odd-odd nuclei, which are always appreciably larger than those of their even-even cores, are in agreement with the assumption that the experimentally determined contributions of the odd neutron and the odd proton to the moment of inertia of the even-even core may simply be added to obtain the moment of inertia of the odd-odd nucleus; in other words, the interaction of the odd proton and neutron does not appreciably affect the moment of inertia. It seemed, therefore, very interesting to study the softness parameter of rotational bands in odd-odd nuclei. The first nucleus, whose rotational band was analyzed (Table IV) Ho^{164}, lies in the strongly deformed region. Its ground state is 1+ and only two excited states are known. It is seen (Table III) that for this nucleus $\mathcal{J}_0$ is $\sim$45% larger than for its even-even core Dy^{162}, and that σ is considerably smaller. Evidence for a rotational band (Table IV) in an odd-odd nucleus which was hitherto considered outside the deformed region, Ir^{194}, may be deduced from a recent result reported by Heiser *et al.*,[46] who found that the multipolarities of the two lowest transitions of 83.5 and 111.0 keV terminating in the 1− ground state are both $M1$. Assuming that

[45] G. Scharff-Goldhaber and K. Takahashi, Bull. Acad. Sci. USSR Phys. Ser. English Transl. **31**, 42 (1967).
[46] C. Heiser, H. F. Brinkmann, and W. D. Fromm, Nucl. Phys. **A115**, 213 (1968).

TABLE V. Intrinsic quadrupole moments Q_{02} and moments of inertia $\mathcal{J}_{02}$ used to determine the constant $k=Q_{02}/(\mathcal{J}_{02})^{1/2}$.

No.[a]	Nucleus	$\mathcal{J}_{02}$[b] (keV^{-1})	Q_{02}[c] (10^{-24} cm^2)
1	Xe^{126}	0.0070	2.80±0.1
2	Xe^{128}	0.0055	2.55±0.4
3	Sm^{150}	0.0070	3.64±0.03
4	Sm^{152}	0.0247	5.85±0.3
5	Sm^{154}	0.0367	6.81±0.14
6	Gd^{152}	0.0067	3.28±0.3
7	Gd^{154}	0.0245	6.08±0.2
8	Gd^{156}	0.0338	6.86±0.15
9	Gd^{158}	0.0376	7.30±0.15
10	Gd^{160}	0.0399	7.55±0.15
11	Dy^{156}	0.0217	6.17±0.3
12	Dy^{158}	0.0303	6.85±0.35
13	Dy^{160}	0.0346	6.91±0.2
14	Dy^{162}	0.0371	7.13±0.1
15	Dy^{164}	0.0408	7.49±0.15
16	Er^{162}	0.0297	7.01±0.15
17	Er^{164}	0.0330	7.23±0.5
18	Er^{166}	0.0371	7.62±0.15
19	Er^{168}	0.0376	7.64±0.15
20	Er^{170}	0.0379	7.46±0.1
21	Yb^{168}	0.0345	7.39±0.15
22	Yb^{170}	0.0356	7.56±0.15
23	Yb^{172}	0.0380	7.77±0.1
24	Yb^{174}	0.0393	7.57±0.1
25	Yb^{176}	0.0365	7.40±0.2
26	Hf^{174}	0.0333	7.27±0.2
27	Hf^{176}	0.0340	7.37±0.15
28	Hf^{178}	0.0321	6.78±0.3
29	Hf^{180}	0.0321	6.73±0.3
30	W^{180}	0.0291	6.65±0.5
31	W^{182}	0.0300	6.46±0.3
32	Os^{186}	0.0219	5.59±0.15
33	Os^{188}	0.0194	5.26±0.2
34	Os^{190}	0.0161	5.06±0.25
35	Pt^{192}	0.0088	5.05±0.25
36	Pt^{194}	0.0085	4.42±0.2
37	Th^{228}	0.0521	8.46±0.4
38	Th^{232}	0.0603	9.87±0.2
39	U^{232}	0.0630	9.98±0.6
40	U^{234}	0.0690	10.0 ±0.4
41	U^{236}	0.0664	10.8 ±0.7
42	U^{238}	0.0670	11.3 ±0.3
43	Pu^{238}	0.0680	10.9 ±0.7
44	Pu^{240}	0.0700	11.3 ±0.2
45	Cm^{244}	0.0699	13.5 ±0.5
46	Pd^{108}	0.0061	2.77±0.15
47	Cd^{110}	0.0036	2.20±0.15
48	W^{184}	0.0270	6.08±0.15
49	W^{186}	0.0245	6.00±0.20

[a] Numbers used in Fig. 9 to identify each nucleus.
[b] The value $\mathcal{J}_{02}=\frac{1}{2}(\mathcal{J}_0+\mathcal{J}_2)$ ($\mathcal{J}_0$ and $\mathcal{J}_2$ are taken from Tables II and I, respectively) (see text).
[c] Values taken from Ref. 4.

they constitute a rotational $K=1$ band, one obtains the parameters given in Table III, which are compared with those of the even-even core nucleus Os^{192}. The results are in good agreement with the regularities stated above and support our conclusion that a rotational band exists in Ir^{194}: $\mathcal{J}_0(Ir^{194})$ exceeds $\mathcal{J}_0(Os^{192})$ by 61% and $\sigma(Ir^{194})$ is 28% smaller than $\sigma(Os^{192})$.

No detailed VMI analysis of rotational bands in odd-A nuclei was undertaken in view of the few bands for which an appreciable number of levels are known. Furthermore, the effect of Coriolis coupling complicates the situation to such a degree[47] that an analysis of this type seems at present futile.

C. Relationship between the Intrinsic Quadrupole Moment and the Moment of Inertia in the Framework of the VMI Model

As mentioned in the Introduction, the large quadrupole moments of 2+ states of even-even nuclei with near-harmonic level schemes are at variance with the spherical nucleus model. On the other hand, the VMI model suggests that the intrinsic quadrupole moments of higher-spin states may be larger than that of the ground state, although the model does not predict any explicit relationship. It is therefore of interest to study Q_I empirically in order to be able to find such a relationship. As a first attempt to study the relationship between Q_I and $\mathcal{J}_I$, we have correlated the values for the transition quadrupole moments Q_{02} obtained from the $B(E2)$ values for the $2+\rightarrow 0+$ transition with the arithmetic mean $\mathcal{J}_{02}=\frac{1}{2}(\mathcal{J}_0+\mathcal{J}_2)$ for $\mathcal{J}$ (Fig. 9, open circles and Table V). The curve represents the function $Q_{02}=k\cdot\mathcal{J}_{02}^{1/2}$, where $k=(39.4\pm 2.6)\times 10^{-24}$ cm^2 keV$^{1/2}$ was obtained by a least-squares fit to the experimental points.[47a] In the same figure the static intrinsic quadrupole moments Q_2 (absolute values) for Sm^{150} [48] and Sm^{152} [49] obtained by means of the reorientation effect are plotted against $\mathcal{J}_2$ (squares). Note that the change of the moment of inertia from $I=0$ to $I=2$ in the "spherical" nucleus Sm^{150} ($\mathcal{J}_0=0.0021$ and $\mathcal{J}_2=0.0128$) given by the VMI model is so large that the value [48] $|Q_2(Sm^{150})| = (4.48\pm 0.6)\times 10^{-24}$ cm^2 falls on the fitted curve. [The corresponding values for the deformed nucleus Sm^{152}, on the other hand, are $\mathcal{J}_0=0.0234$, $\mathcal{J}_2=0.0260$, and $|Q_2| = (6.3\pm 2.1)\times 10^{-24}$ cm^2.[49]] (Unfortunately, the other cases for which Q_2 values have been measured cannot be shown on this figure, since no ground-state band including at least a 6+ state is known for the nuclei in question.) This result indicates that on the basis of the VMI model near-harmonic nuclei may very

[47] C. W. Reich and M. E. Bunker, Bull. Acad. Sci. USSR Phys. Ser. English Transl. **31**, 46 (1967).

[47a] The puzzling fact, observed by L. Grodzins [Phys. Letters **2**, 88 (1962)], that the proportionality factor between the reduced transition probability $B(E2;\ 2\rightarrow 0)$ and $1/E_2$ is the same for "vibrational" and deformed nuclei, thus appears quite plausible from the point of view of the VMI model.

[48] J. J. Simpson, D. Eccleshall, N. J. L. Yates, and N. J. Freeman, Nucl. Phys. **A94**, 177 (1967).

[49] G. Goldring and U. Smilansky, Phys. Letters **16**, 151 (1965).

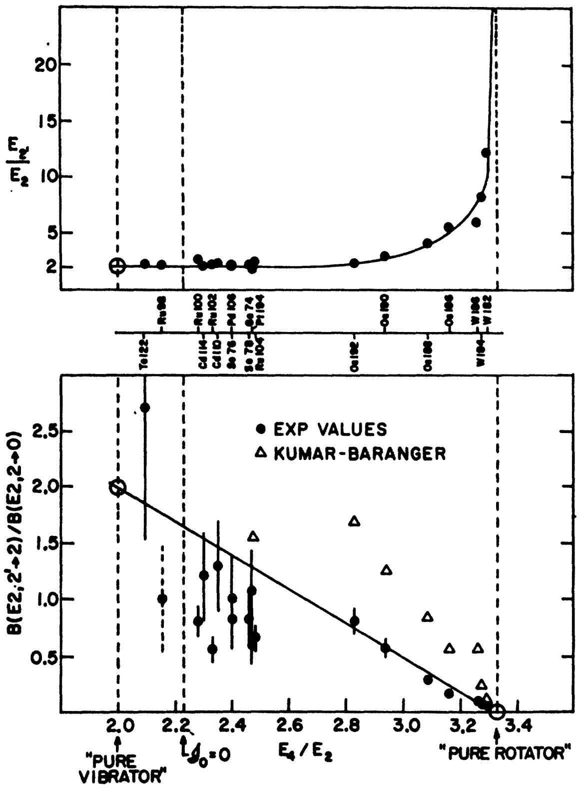

FIG. 10. Ratios $E_{2'}/E_2$ of the energies of the second to the first 2+ states (above) and the ratios of reduced transition probabilities $B(E2, 2'\rightarrow2)/B(E2, 2\rightarrow0)$ (Refs. 8–12) (below) plotted versus E_4/E_2. Experimental points are indicated with solid circles. In the lower plot the values predicted by Kumar and Baranger (Ref. 50) are shown with open triangles. The straight line drawn in the lower part connects the predictions of the pure vibrational and rotational models. In the upper part the line has been drawn through the experimental values to guide the eye.

well have appreciable quadrupole moments in the 2+ state, as $\mathcal{J}_2 \gg \mathcal{J}_0$, while the intrinsic quadrupole moments of the ground state are very small. At present half-life measurements of states within rotational bands are being undertaken[6] by means of Doppler shift methods. It will be very interesting to see whether the relationship shown in Fig. 9 holds also for the higher-lying states.

D. Correlation between Nuclear Softness and the Ratio of Reduced Transition Probabilities $B(E2)(2'\rightarrow2)/B(E2)(2\rightarrow0)$

It was pointed out in the Introduction that, for a truly vibrational nucleus,

$$B(E2)(2'\rightarrow2)/B(E2)(2\rightarrow0)=2.$$

However, most of the experimental values measured for this quantity are appreciably smaller.[8–12] It had been shown[8] previously that the predictions from the asymmetric model[15] agree fairly well with the experimental values, but that at the same time the 4+ states predicted by this model are too high. In order to study the correlation of the $B(E2)$ ratio with the softness parameter, we have plotted this quantity (full circles) as a function of E_4/E_2, which, in turn, is a function of σ only (Fig. 10) (see Sec. II C). The open circles, connected by a straight line, indicate the theoretical values for vibrational nuclei and for rigid rotators. The points for the Os and W nuclei lie close to this straight line, while the points for the near-harmonic nuclei (Ge, Se, Ru, Pd, Cd, and Pt) scatter around a value of ~1. The value for Te^{122} for which E_4/E_2 lies below the region of validity of the VMI model appears to be at least as high as the interpolated value. The authors of Ref. 10 point out, however, that several sources of possible errors are not included in the error bars given, among them, a possible difference between Q_0 and Q_2. For a comparison we have indicated the Kumar-Baranger predictions[50] (triangles). It appears that the softness parameter is definitely correlated with the $B(E2)$ ratio under consideration. In the upper part of the figure the ratios $E_{2'}/E_2$ are presented which show a smooth dependence on E_4/E_2.

IV. SUMMARY

The VMI model proposed here is independent of the particular way (e.g., β stretching, decrease in pairing energy) in which the variation of $\mathcal{J}$ takes place. By means of this model the extended ground-state bands ($0\leq I\leq16$) of 88 nuclei ranging from Pd to Cm have been calculated with two adjustable parameters, $\mathcal{J}_0$ and σ. Both parameters, presented as functions of N and Z (Figs. 7 and 8), are shown to vary smoothly: $\mathcal{J}_0$ reaches the highest and σ the lowest values at the stability line for nuclei furthest removed from magic proton and neutron numbers. The situation is reversed when magic numbers are approached. The parameters show rapid changes between 88 and 90 neutrons, high values for both $\mathcal{J}_0$ and σ are reached at 98 neutrons, and breaks are found for 104, 108, and 110 neutrons. Most of these breaks are paralleled by breaks in the two neutron binding energies. The variations of the parameters for the Os and Pt nuclei are of particular interest.

Parameters of bands built on γ-vibrational states in even-even nuclei and of bands found in odd-odd nuclei are closely related to the parameters of ground-state bands in the appropriate even-even nuclei. Mallmann's empirical "universal curves" have been deduced from the VMI model for $E_4/E_2>2.23$. It was further shown that the VMI model is mathematically equivalent to the two-parameter Harris model.

---

[50] M. Baranger (private communication).

An empirical relationship between static and transition quadrupole moments on one hand and the variable moment of inertia on the other has been obtained. The ratios E_2'/E_2 and $B(E2, 2'\rightarrow 2)/B(E2, 2\rightarrow 0)$ were found to be related to E_4/E_2, and thus to σ.

It could further be shown that even a band of a nucleus displaying a particularly complex behavior in terms of the microscopic analysis of Kumar and Baranger,[43] such as Pt^{194}, is accurately described by the VMI model.

In view of the foregoing, it may be expected that an analysis of the two parameters ($\mathcal{I}_0$ and σ) obtained from this one-variable ($\mathcal{I}$) model will lead to greater insight into nuclear dynamics.

ACKNOWLEDGMENTS

We are indebted to Dr. D. Bes, Dr. S. Kahana, Dr. A. K. Kerman, Dr. S. G. Nilsson, Dr. W. T. Swiatecki, Dr. A. Zuker, and especially Dr. J. Weneser for enlightening discussions. Our thanks are also due to Dr. Diamond, Dr. Stephens, and Dr. Ward and to Dr. P. H. Stelson and Dr. F. K. McGowan for frequent private communications of their data. We further wish to thank Dr. M. Baranger and Dr. K. Kumar for private communications of their results. Finally, we should like to thank Dr. R. Marr and Dr. P. Thieberger for their helpful advice concerning the numerical calculations.

PHYSICAL REVIEW VOLUME 178, NUMBER 4 20 FEBRUARY 1969

Production of In^{111} and In^{114m} from the Separated Isotopes of Cadmium Using 70- to 400-MeV Protons*†

W. J. Nieckarz, Jr.,‡ and A. A. Caretto, Jr.
Carnegie-Mellon University, Pittsburgh, Pennsylvania 15213

(Received 26 September 1968)

The cross sections for the $Cd^{110+x}(p, xn)In^{111}$ and the $Cd^{113+x}(p, xn)In^{114m}$ reactions at proton energies from 70 to 400 MeV have been measured using the separated isotopes of cadmium as targets. The energy dependence of the (p, n), $(p, 2n)$, and $(p, 3n)$ reactions is inversely proportional to the incident energy over the entire energy region, while the $(p, 4n)$ and $(p, 6n)$ reactions exhibit this energy dependence only above 150 MeV. This similar energy dependence of the (p, xn) reactions supports the conclusion that these reactions take place by the same mechanism: a p-n cascade step followed by the evaporation of $x-1$ neutrons. The change in the energy dependence of the $(p, 4n)$ and $(p, 6n)$ reactions below 100 MeV is probably due to contributions from compound-nucleus processes. The experimental results are compared with Monte Carlo cascade and evaporation calculations.

INTRODUCTION

The production of In^{111} and In^{114m} was studied as a function of incident proton energy from targets consisting of the separated cadmium isotopes. Unlike other studies of (p, xn) reactions which generally involve the production of a different product from the same target with each change in x, in this work the production of the same products In^{111} and In^{114m} from the separated target isotopes of cadmium eliminates uncertainties in decay schemes and detection methods in the calculation of relative cross sections.

As discussed by Church and Caretto[1], the most plausible mechanism for (p, xn) reactions involves a $(\tilde{p}, \tilde{n})$ cascade[2] leading to sufficient residual excitation energy such that $(x-1)$ neutrons can be evaporated. Since the evaporation process is sensitive to nucleon binding energies, Coulomb barriers, and shell effects, while the cascade is generally insensitive to these effects, the results of the study of the type of (p, xn) reactions reported here should be nearly exclusively dependent on the cascade part of the interaction.

Thus, the mechanism should involve a p-n scattering or charge exchange such that the proton is scattered at large center of mass angles for (p, n) reactions. The residual excitation energy E^* is given by $E^*= E_p+E_f-E_j$, where E_p is the recoil kinetic energy of the proton scattered through a center-of-mass scattering angle θ near 180°, E_f the nucleon kinetic energy at the top of the Fermi sea, and E_j the neutron kinetic energy prior to collision. In order that E^* be large enough so that $x-1$ neutrons are energetically allowed

* This research was performed under a contract with the U.S. Atomic Energy Commission.

† Presented in partial fulfillment of the requirements of the Ph.D. degree in the Department of Chemistry, Carnegie Institute of Technology, Pittsburgh, Pa. 15213.

‡ Present address: Department of Chemistry, Wisconsin State University, LaCrosse, Wisc. 54601.

[1] L. B. Church and A. A. Caretto, Jr., Phys. Rev. **178**, 1732 (1969).

[2] Specific nucleonic cascades are represented by letters with tildes, such as $(\tilde{p}, \tilde{n})$, $(\tilde{p}, 2\tilde{n})$, etc. The over-all nuclear reaction is designated by the plain letters.